

September 2015

# Ductility and Use of Titanium Alloy and Stainless Steel Aerospace Fasteners

Jarrold Talbott Whittaker

University of South Florida, jarrod1@mail.usf.edu

Follow this and additional works at: <http://scholarcommons.usf.edu/etd>

 Part of the [Aerospace Engineering Commons](#), [Materials Science and Engineering Commons](#), and the [Mechanical Engineering Commons](#)

## Scholar Commons Citation

Whittaker, Jarrold Talbott, "Ductility and Use of Titanium Alloy and Stainless Steel Aerospace Fasteners" (2015). *Graduate Theses and Dissertations*.

<http://scholarcommons.usf.edu/etd/5796>

This Thesis is brought to you for free and open access by the Graduate School at Scholar Commons. It has been accepted for inclusion in Graduate Theses and Dissertations by an authorized administrator of Scholar Commons. For more information, please contact [scholarcommons@usf.edu](mailto:scholarcommons@usf.edu).

Ductility and Use of Titanium Alloy and Stainless Steel Aerospace Fasteners

by

Jarrold Talbott Whittaker

A thesis submitted in partial fulfillment  
of the requirements for the degree of  
Master of Science in Mechanical Engineering  
Department of Mechanical Engineering  
College of Engineering  
University of South Florida

Major Professor: Daniel P. Hess, Ph.D.  
Wenjun Cai, Ph.D.  
Nathan Crane, Ph.D.

Date of Approval:  
July 29, 2015

Keywords: A286, Ti 6Al-4V, Tensile Testing, Ductility Index, Joint Diagram

Copyright © 2015, Jarrod Talbott Whittaker

## DEDICATION

I would like to dedicate this thesis to my grandpa Frank and grandpa Clyde along with my mom and dad. I thank my grandpa Frank for all his support allowing me, and encouraging, me to obtain this degree and my grandpa Clyde for showing me what all can be achieved with a Master's degree in Engineering. I would not be the person I am today without the balance of both my parents with their love and encouragement to pursue this degree. I thank you all for all your hard work and dedication to our family, you have truly been an inspiration to me throughout my life as people who I admire and look up to. I thank the rest of my family for always checking up on how my thesis was progressing and being interested in my endeavors. Lastly, I thank all my friends for making this time the best couple years of my life so far and especially Alan for being there every step of the way with me in the lab. It would have not been nearly as fun without you.

## ACKNOWLEDGMENTS

I would like to recognize Dr. Daniel Hess my major thesis professor for allowing me to work with him and giving me a really fun and interesting research project as well as for getting our NASA funding. I thank my two committee members Dr. Wenjun Cai and Dr. Nathan Crane for answering any questions I had and giving me feedback during my defense. A big thank you to Kevin Johnson in the structures lab for giving me so much help during my tensile testing. Thank you as well to Yari and Judy in the Mechanical Engineering office for always being eager to help, keeping me on track with deadlines, and for ordering my test materials. A thank you as well to Tony and Chester in the machine shop for getting all my test fixtures made so quickly during testing.

## TABLE OF CONTENTS

LIST OF TABLES .....	iii
LIST OF FIGURES .....	iv
ABSTRACT.....	vii
CHAPTER 1: INTRODUCTION.....	1
CHAPTER 2: BACKGROUND.....	4
CHAPTER 3: TESTING .....	10
3.1 Test Specimens .....	10
3.2 Tensile Testing Machine.....	11
3.3 Test Procedure and Setup.....	12
CHAPTER 4: RESULTS.....	17
4.1 Fastener Strength .....	17
4.2 Ductility Index .....	20
CHAPTER 5: EXAMPLE PROBLEMS .....	25
5.1 Joint Design .....	25
5.2 Bolted Joint Diagram Values.....	29
5.3 Constructing a Joint Design Example.....	30
5.4 Interpreting a Joint Design Example.....	31
5.5 Using the Joint Diagram .....	32
5.6 Joint Diagram Examples .....	34
5.7 90% Yield Preload with +/- 25% Uncertainty from Torque.....	35
5.7.1 115% Preload with A286.....	36
5.7.2 115% Preload with Titanium 6-4.....	37
5.7.3 90% Preload with A286.....	38
5.7.4 90% Preload with Titanium 6-4.....	39
5.8 65% Yield Preload with +/- 25% Uncertainty from Torque.....	40
5.8.1 65% Preload with A286.....	40
5.8.2 65% Preload with Titanium 6-4.....	42
5.9 65% Yield Preload with +/- 25% Uncertainty from Torque and Full Loading Planes .....	42

5.9.1 90% Preload with A286 and Full Loading Planes .....	43
5.9.2 90% Preload with Titanium 6-4 and Full Loading Planes .....	44
5.9.3 65% Preload with A286 and Full Loading Planes .....	45
5.9.4 65% Preload with Titanium 6-4 and Full Loading Planes .....	46
CHAPTER 6: DISCUSSION.....	47
6.1 Tensile Test Data .....	47
6.2 Ductility Index .....	48
6.3 Joint Diagram Examples .....	49
CHAPTER 7: CONCLUSIONS .....	52
REFERENCES .....	54
APPENDIX A: HEAT TREATMENTS.....	57
A.1 A286 Heat Treatment.....	57
A.2 Titanium 6-4 Heat Treatment.....	57
APPENDIX B: CHOICE OF SAMPLE SIZE.....	60
APPENDIX C: DUCTILITY INDEXES .....	63
C.1 Titanium 6-4 Ductility Index.....	63
C.2 A286 Ductility Index.....	69
APPENDIX D: SPRING CONSTANT CALCULATIONS .....	77
D.1 Bolt Spring Constant.....	77
D.2 Joint Spring Constant.....	78
APPENDIX E: JOINT DIAGRAM CALCULATIONS .....	80
APPENDIX F: OTHER JOINT DIAGRAM EXAMPLES.....	83
APPENDIX F: COPYRIGHT PERMISSION.....	91

## LIST OF TABLES

Table 1 - Fastener Material Number .....	12
Table 2 - Randomized Run Sequence .....	13
Table 3 - Fastener Yield Strengths.....	19
Table 4 - Average Ductility Index .....	21
Table 5 - Preload Scenario Loadings .....	30
Table 6 - Joint Diagram Examples.....	35
Table 7 - Joint Diagram Example Results .....	50
Table A - Titanium 6Al-4V Bolt Manufacturing Procedure .....	58
Table B - Ductility Index Calculations .....	75

## LIST OF FIGURES

Figure 1: Ti-6Al-4V Phase Diagram.....	5
Figure 2: A286 Stress Strain Curves.....	8
Figure 3: Ti 6Al-4V Stress Strain Curves.....	9
Figure 4: A286 and Ti 6Al-4V Test Specimens .....	10
Figure 5: 220 Kip MTS Tensile Testing Machine .....	12
Figure 6: MTS Gripper with Tensile Specimen Ready for Testing.....	14
Figure 7: Custom Test Fixtures, Gripper, Washer, and Fasteners .....	16
Figure 8: A286 Load vs. Displacement Tests.....	17
Figure 9: Titanium 6Al-4V Load vs. Displacement Tests.....	18
Figure 10: A286 & Titanium 6Al-4V Load vs. Displacement .....	18
Figure 11: Yield Strengths for Titanium 6Al-4V and A286.....	19
Figure 12: Ductility Index Quantification.....	21
Figure 13: Titanium 6-4 Fastener Failure .....	22
Figure 14: A286 Fastener Failure .....	22
Figure 15: Joint Diagram with Applied External Load .....	26
Figure 16: Bolted Joint with Loading Planes.....	27
Figure 17: Joint Diagram Loading Plane Effects.....	28
Figure 18: Joint Diagram Naming Convention.....	31
Figure 19: NASA 5020 Joint Separation Flow Chart [7] .....	33



Figure 20: 115% Preload of A286 Joint Diagram .....	36
Figure 21: 115% Preload of Titanium 6-4 Joint Diagram .....	37
Figure 22: 90% Preload of A286 Joint Diagram .....	38
Figure 23: 90% Preload of Titanium 6-4 Joint Diagram .....	39
Figure 24: 65% Preload of A286 Joint Diagram .....	41
Figure 25: 65% Preload of Titanium 6-4 Joint Diagram .....	42
Figure 26: 90% Preload of A286 Joint Diagram – Full Load Planes .....	43
Figure 27: 90% Preload of Titanium 6-4 Joint Diagram – Full Load Planes .....	44
Figure 28: 65% Preload of A286 Joint Diagram – Full Load Planes .....	45
Figure 29: 65% Preload of Titanium 6-4 Joint Diagram – Full Load Planes .....	46
Figure 30: Representative Load vs. Displacement Graphs .....	47
Figure A: Titanium 6Al-4V Grain Structure with Heat Treatment .....	59
Figure B: Operating Characteristic Curve [31].....	60
Figure C: Titanium 6-4 Ductility Index Specimen 1 .....	63
Figure D: Titanium 6-4 Ductility Index Specimen 2 .....	64
Figure E: Titanium 6-4 Ductility Index Specimen 3 .....	64
Figure F: Titanium 6-4 Ductility Index Specimen 4.....	65
Figure G: Titanium 6-4 Ductility Index Specimen 5 .....	65
Figure H: Titanium 6-4 Ductility Index Specimen 6 .....	66
Figure I: Titanium 6-4 Ductility Index Specimen 7.....	66
Figure J: Titanium 6-4 Ductility Index Specimen 8 .....	67
Figure K: Titanium 6-4 Ductility Index Specimen 9 .....	67
Figure L: Titanium 6-4 Ductility Index Specimen 10 .....	68

Figure M: Titanium 6-4 Ductility Index Specimen 11 .....	68
Figure N: Titanium 6-4 Ductility Index Specimen 12 .....	69
Figure O: A286 Ductility Index Specimen 13 .....	69
Figure P: A286 Ductility Index Specimen 14.....	70
Figure Q: A286 Ductility Index Specimen 15 .....	70
Figure R: A286 Ductility Index Specimen 16 .....	71
Figure S: A286 Ductility Index Specimen 17.....	71
Figure T: A286 Ductility Index Specimen 18.....	72
Figure U: A286 Ductility Index Specimen 19 .....	72
Figure V: A286 Ductility Index Specimen 20 .....	73
Figure W: A286 Ductility Index Specimen 21 .....	73
Figure X: A286 Ductility Index Specimen 22 .....	74
Figure Y: A286 Ductility Index Specimen 23 .....	74
Figure Z: A286 Ductility Index Specimen 24.....	75
Figure AA: Joint Diagram Naming Convention.....	80
Figure BB: 40% Preload of A286 Joint Diagram .....	83
Figure CC: 40% Preload of Titanium 6-4 Joint Diagram .....	84
Figure DD: 40% Preload of A286 Joint Diagram - Full Loading Planes .....	85
Figure EE: 40% Preload of Titanium 6-4 Joint Diagram - Full Loading Planes .....	86
Figure FF: 65% Preload of A286 Joint Diagram .....	87
Figure GG: 65% Preload of Titanium 6-4 Joint Diagram.....	88
Figure HH: 90% Preload (65%+25% Uncertainty) of A286 Joint Diagram .....	89
Figure II: 90% Preload (65%+25% Uncertainty) of Titanium 6-4 Joint Diagram .....	90

## ABSTRACT

The main purpose of this thesis is to investigate the ductility and application of titanium alloys, like titanium 6Al-4V, when used in aerospace fasteners compared to more conventional stainless steel aerospace fasteners such as A286. There have been concerns raised about the safe usability of titanium 6-4 in the aerospace industry due to its lack of strain hardening. However, there is a lack of data pertaining to this concern of safe usage which this thesis aims to address. Tensile tests were conducted to find the ductility indexes of these fasteners which quantify the amount of plastic to elastic elongation. From the tests conducted it was found that the two materials yield and tensile strengths were very similar, though the ductility index of A286 is on average ten times greater than that of titanium 6-4. This thesis includes joint diagram examples that analyze typical joints using both materials. It was found from joint diagram examples that the lower ductility index of the titanium alloy will only be detrimental to use at higher preloads. However, the titanium alloy can be used safely in place of A286 in most loading situations just with narrower safety margins in these controlled examples.

## CHAPTER 1: INTRODUCTION

In the aerospace and aeronautical fields mass is almost always the enemy; increasing costs for launch or flight and decreasing vehicle performance, every kilogram matters in the design. How much weight could be saved in a design if the mass of every fastener on a satellite bus or airplane could be cut in half while still maintaining safety? That is the question that the titanium alloy Ti 6Al-4V is posing to the more widely utilized stainless steel alloy A286.

Titanium has many uses in a variety of fields due to its many desirable characteristics. There are four grades of commercially available pure titanium and six grades of titanium alloys [1]. This material and its various alloys are utilized primarily in the aerospace and aeronautics industry because of its good strength to weight ratio compared to steels [2,3]. The density of the titanium alloy is almost half that of A-286 stainless steel at 4.43 g/cc compared to the steels 7.916 g/cc [4]. Titanium has found extensive use in the biomedical field as well because of its lack of biological response in the human body. A few more notable applications of this metal and its alloys are in the chemical, industrial, and marine industries because of its excellent corrosion resistance, even at elevated temperatures. The alloys show almost no signs of corrosion that would cause failure if the proper coating were applied for its operating field [5,6]. The most prevalent version of commercially pure titanium is grade 2 and it is used in most titanium bar and sheet stock. The most well used version of titanium in the world is grade 5 titanium or Ti-6Al-4V. This grade of titanium is what will be the focus of this paper. All the

previously mentioned applications primarily use Ti-6Al-4V as well, though an alloy without Vanadium is gaining usage in the medical field. This Ti-6Al-4V alloy is called the “workhorse” of the titanium industry and accounts for over 50 percent of the total titanium usage worldwide. This alloy can be solution treated, and age hardened to increase its strength and fracture toughness while withstanding service temperatures of up to 600 degrees Fahrenheit.

The idea behind this project is to provide data through tensile testing that can allow engineers to draw conclusions about the safe usage of this alloy in aerospace fastener applications. This investigation will be through the use of an MTS tensile testing machine to investigate the ductility index of this alloy in full size fastener specimen form compared to A286 fasteners of the same dimensions. From these results the ductility index can be determined in accordance to NASA standard 5020 [7]. From this tensile test data, conclusions can be drawn to see if the concerns of the titanium alloy being too brittle for fastener use are founded. The characteristic of ductility of the Ti-6Al-4V alloy when used in fasteners has not had sufficient research so that is the aim of this project. Since the aerospace and aeronautical engineering fields have such high performance criteria it is necessary to try and find out as much as possible with regard to ductility of this fastener to see if it could and should be used more prevalently in these fields, or to show how it can be more carefully utilized. Hopefully, this paper will provide a clearer understanding of how this material can be more safely used in these applications as well as the other fields previously mentioned. Either good or bad, a more informed decision can be made when deciding on a design that utilizes Ti-6Al-4V fasteners.

The plan is to gather load and displacement data through tensile testing. This will provide ductility indexes for titanium compared to A286. The ductility index is widely used for bolted joint testing, Fiber Reinforced Concrete Beams, and other instances where direct tensile testing

with machined tensile specimens cannot be performed but an idea of ductility needs to be known [8-16]. In this thesis, ductility index will be used for full size fastener specimen testing as suggested by Dolan in his paper suggesting a testing method to be reviewed by ASTM for this very purpose [16]. Ductility index can be computed simply from the force vs. displacement graph pulled from the tensile test. It is referred to as the ratio of displacement between yield and max tensile load over displacement at yield and will be explained more fully later in this thesis [17-19]. Chapter 5 of this thesis will also be dedicated to loading scenarios for joint design with different preload and external load levels. These examples will allow engineers to more fully understand bolted joint design and provide suggestions for applications where the titanium alloy can be trusted to perform as well as the A286 thus providing a light weight design while still maintaining safety.

## CHAPTER 2: BACKGROUND

The focus of this paper will be on the use of Ti-6Al-4V bolts in the aerospace industry. This titanium alloy as mentioned earlier is the “workhorse” of the industry accounting for 50% of the titanium in use worldwide. Ti-6Al-4V is an alpha-beta alloy. Alpha-beta alloys contain limited amounts of beta stabilizers, which cannot strengthen the alpha phase and therefore need alpha stabilizers as well. Hexagonal Close Packed (HCP) Alpha phase, and Body Centered Cubic (BCC) Beta phases are the two allotropes of titanium. This alloy contains aluminum, as its alpha stabilizer along with some small amounts of Oxygen while Vanadium is the beta stabilizer. The final microstructure of this alloy depends on the heat treatment processing the fastener goes through. This microstructure, and therefore mechanical properties, is governed by the distribution of alpha and beta phases in the alloy, which is controlled by the variation in heat treatment regimes. This alloy is called an Alpha-Beta alloy because it retains the high temperature beta phase at room temperature after the heat treatment process has taken place. The most important line to note is the beta transus temperature line, which can be seen in Figure 1 below [20]. This transition temperature for the alloy is around 995 degrees Celsius and is where the alloy’s microstructure transforms from HCP (Alpha) to BCC (Beta) structure.

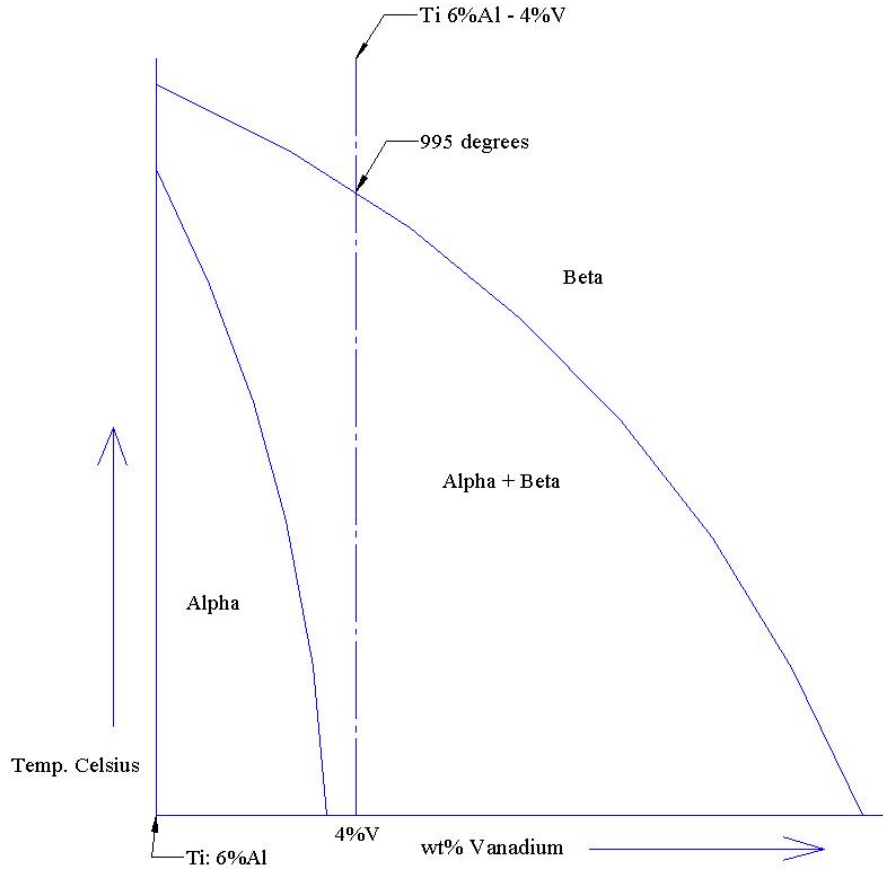


Figure 1: Ti-6Al-4V Phase Diagram. Adapted from [20]

Heat treatment in the beta phase leads to different mechanical characteristics after being cooled from this treatment temperature. An adverse effect is a significant decrease in ductility. However, working above the beta transus temperature increases fracture toughness. Therefore, a final heat treatment such as age hardening will usually take place in the alpha + beta region to gain back some loss of ductility. The titanium alloy fasteners used in testing went through a heat treatment process below the Beta transus temperature however. To obtain high strength with adequate ductility solution treatment temperature of the fasteners used was at 932 degrees Celsius with age hardening at 510 degrees Celsius. The basis of either heat treatment process above or below the beta transus temperature is to increase the amount of the stronger beta phase



within the alloy. When the solution treatment temperature is below the Beta transus, like the fasteners used in testing, the beta phase decomposes in the age hardening treatment and provides the higher strength to the material. All heat treatment details for both fasteners are in Appendix A.

This titanium alloy is spaceflight approved, but has a “checkered” history during use in the space as well as aeronautics industry [21]. In some applications failure of these bolts were due to material defects [17,18]. However, most were deemed to be failures caused by inadequacies in the method and specifications of installation [21,19]. These failures during install might bridge from a lack of information as to the proper preload values to use in these fasteners since this alloy’s mechanical characteristics differ from the more widely used A286 stainless steel.

As stated previously this increase in strength comes at the price of being less ductile. This brittleness in the material is what has caused the “checkered” history of this material when used in fastener applications. The previous reports on bolt failure with this material show the shank of the bolt failed perpendicular to its axis, which is indicative of a brittle material failure when the applied force is in tension.

These failures can come from many factors. The uncertainty in the amount of preload on the fastener from the applied tightening torque is one reason. This failure comes from the complicated relationship of knowing the true stress in the bolt when subjected to some applied torque. The effective elasticity of the fastener as well as joint elasticity plays an important role on the stress seen in the fastener. These factors along with the joints loading planes make it difficult to know the preload on the fastener [22]. Another reason for premature failure is caused by not applying the proper lubricant on the threads of the fastener. Lubricant is always needed

for nominal and repeatable results in testing as well as in service. Some more factors that apply to properly functioning bolted joints are correct joint design and adequate bolt preload. These two factors can be just as important as the fasteners yield and tensile strength [23]. The proper joint design along with maintaining adequate preload on the joint will help to ensure proper function during service. Some real world joint problems will be in Chapter 5 of this thesis. The proper preload during service along with material choices will make sure that the joint, and not the fastener, will take the majority of the energy of the system. It has been shown that a relatively elastic bolt with a stiff clamped material is the best design. This will minimize preload loss and dynamic bolt loads, as well as make sure the clamped material takes the energy and not the bolt.

As stated, steel fastened joints can safely be tightened up to and beyond their yield strength [23]. This technique has the advantage of ensuring the maximum preload the bolt can handle is achieved and knowing exactly how much load the bolt has on it once fastened. This, however, provides a possible problem in the case of Ti-6Al-4V. This material is thought not to have enough strain hardening capabilities, compared to its aerospace grade steel counterparts, like A-286, to be able to absorb much more stress after it reaches its yield point. With little strain hardening of Ti-6Al-4V this might not be a safe method to achieve a functioning joint [20]. The stress-strain curves of A-286 and Ti-6Al-4V can be seen in figures 2 and 3 at several strain rates.

This lack of strain hardening before failure is the biggest drawback of the titanium alloy compared to its A286 counterpart for the aerospace and aeronautics industries. It has been suggested up to this point to only use the titanium alloy when the weight savings are critical and preferably when a titanium fastener is not the only point of failure [21]. The yield strength of the titanium alloy is higher than that of the A286 at all strain rates from the compression tests shown below [24,25]. However, once the yield strength of the titanium alloy is reached it is not able to

withstand much more load and reaches its ultimate tensile strength. In the case of the titanium alloy it is thought there is not much room for error in expected external loads in the joint and the amount of preload on the bolt needs to be carefully considered by taking out as much error from the torque-tension relationship as possible.

The stress-strain graphs shown in Figures 2 and 3 are the best found for Ti-6Al-4V and A286 during research and come from a United Air Force Study of aerospace materials. [24] Since these results are compression tests using a Split Hopkins Bar Apparatus it shows that not enough research on this titanium alloy for fastener applications has been completed since that is the best that could be found as far as stress-strain data and therefore why this research will utilize a tensile test of the fastener specimens. This lack of relevant data for the alloy in a fastener application is the main reason for this research since it is gaining more popularity in the aforementioned fields. Bar stock testing and titanium alloy in sheets are the only other specimens found in papers. The only research papers that dealt with this alloy in fasteners were for after the bolt had already failed and the research was for finding out why it broke [20,17,18]

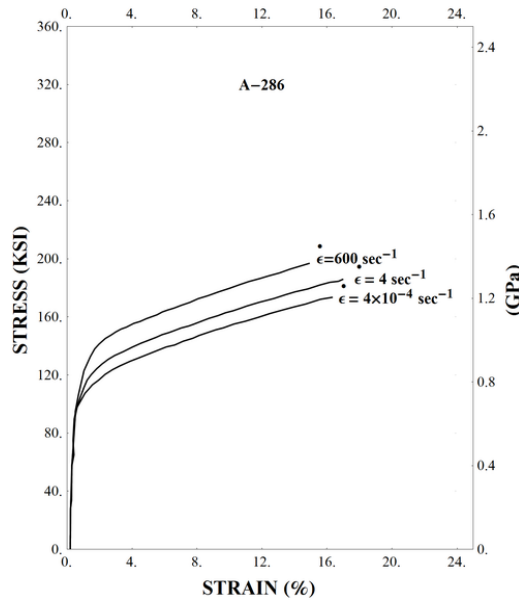


Figure 2: A286 Stress Strain Curves. Pulled from a public source [24]

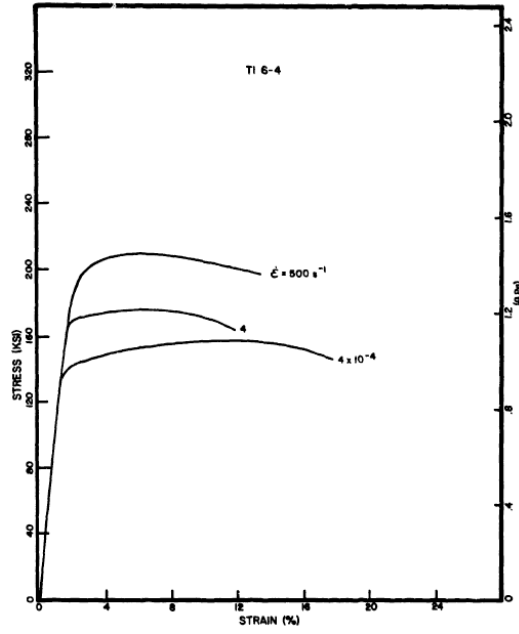


Figure 3: Ti 6Al-4V Stress Strain Curves. Pulled from a public source [24]

## CHAPTER 3: TESTING

### 3.1 Test Specimens

The tensile testing conducted compares Titanium 6-4 to A286. They are both quarter inch diameter bolts of two-inch length (1.99 inches for Ti 6-4, and 2.03 inches for A286 with similar threaded lengths) with UNJF threads for consistency. The only visual difference is in the design of the bolt head with the titanium being a 12 point head and the A286 the usual hex configuration. This difference did not affect the testing however since the failure was in the thread of the bolts. The lot of titanium was from an aerospace fastener company who sent the full processing history of the bolts and are capable of meeting AMS 4928 Rev: R and 4967 Rev: J specifications. The A286 fasteners are NAS 1004-24A spec and came with the full certification sheet from the bar stock manufacture through heat treatments, forging/machining, and proof testing. These specifications are in Appendix A and the two fasteners can be seen in Figure 4 below.



Figure 4: A286 and Ti 6Al-4V Test Specimens

### 3.2 Tensile Testing Machine

To investigate fastener properties the tensile testing machine utilized is a 220 Kip load frame MTS unit. Load cell is MTS part number 390751-03, and serial number 620094. A tensile calibration test was done just before testing with a 20 kip S Type load cell to verify calibration numbers. The lab manager gave a full tutorial on MTS operations before testing was conducted and oversaw the preliminary testing and first few runs. Data collection was exported through an Omega USB Data Acquisition Module with model number OMB DAQ56 to a separate laptop. The force and displacement data with respect to time were setup to populate an Excel sheet for each test on the laptop and a new sheet was started for each run. The machine well exceeds the tensile capabilities needed to perform this tension test but the load cell can be set to a 22 Kip (i.e. 22,000 lbs.) setting making data recording more accurate. A picture of the MTS tensile testing machine is in figure 5 below. The machine's cross bar was brought down so that the range of displacement from the hydraulic ram was enough to perform a proper tensile test to ASTM F606-02 specs of 2 kips/minute for these specimens [26]. In this MTS machine the cross bar on top stays static while the ram in the bottom of the machine provides the loading. The MTS gripper for holding the head of the specimens is also shown in the figure in testing configuration. A donut shaped adapter was made for our testing procedure from the University's machines shop. The outer diameter screws fully into the hydraulic cross-head of the MTS machine while the inner diameter is threaded to fit the grippers used. Further details of the test fixtures will follow in the next section.



Figure 5: 220 Kip MTS Tensile Testing Machine

### 3.3 Test Procedure and Setup

The testing order of the 24 test fasteners seen in Table 1 was randomized using a random number generator. The randomized test order can be seen in Table 2. The twenty four fasteners were visually inspected and sprayed with dry moly lubricant and allowed to fully dry then placed in a sectioned off container and labeled by fastener number. When the fasteners number came up in the test order it was picked out of the container for testing and once fractured it was placed back into its cell.

Table 1- Fastener Material Number

Material:	Fastener Material Number
Titanium 6-4	1 2 3 4 5 6 7 8 9 10 11 12
A286	13 14 15 16 17 18 19 20 21 22 23 24

Table 2- Randomized Run Sequence

Fastener Number	Test Order	Material Order
1	6	Titanium 6-4
2	2	Titanium 6-4
3	12	Titanium 6-4
4	8	Titanium 6-4
5	21	A286
6	7	Titanium 6-4
7	17	A286
8	20	A286
9	13	A286
10	11	Titanium 6-4
11	24	A286
12	5	Titanium 6-4
13	9	Titanium 6-4
14	15	A286
15	18	A286
16	10	Titanium 6-4
17	4	Titanium 6-4
18	23	A286
19	14	A286



Table 2 (Continued)

20	19	A286
21	16	A286
22	1	Titanium 6-4
23	22	A286
24	3	Titanium 6-4



Figure 6: MTS Gripper with Tensile Specimen Ready for Testing

In Figure 6 the gripper is used to hold the head of the test specimen for tensile testing in the MTS machine. The gripper is rated to 60,000 pounds, which is well above the yield strengths

calculated for our test specimens which are all less than 6,200 pounds. The MTS crossbar head was adjusted and then locked in place so that the hydraulic ram below had enough range of motion to fracture the specimen. The hydraulic ram in the base of the machine provides the loading and has the other custom-made test fixture. The outside diameter is threaded into the ram and the inner diameter was drilled and tapped so that the test specimens can be threaded directly into it with consistent full thread engagement over all the tests. A non-tapped hole was drilled all the way through this 1.6 inch thick test fixture, as can be seen on the right of figure 7 below, and then the top 3/8" was tapped. This 3/8" provides full thread engagement and ensures that all the test specimens had the same thread engagement. There is a 3/8" thick testing puck with a 1/4" diameter hole in the center which comes with the gripper and was used under the head of the bolt during testing. This puck sits in a recessed circular area in the gripper and ensures that a pure axial load is applied to the fastener. This test setup was used instead of a bolt with a nut and another gripper in the hydraulic ram to take out any extra elongation effects from the nut and the extra threaded interfaces of the second gripper's adapter. This test configuration was thought to best isolate and test the bolts capabilities and are why ASTM F606 and NASA STD-5020 were deviated from for this test. These fixtures can be seen in Figure 7 at the end of this chapter.

To setup the specimen for testing it was placed through the testing washer and then the washer was placed in the gripper's recessed circular area. From there the ram was brought up so that the bolt could be fully threaded until it bottomed out in the test fixture in the ram. The ram was slowly lowered until no gap between the washer and head could be seen. From there a 100 pound preload was placed on all of the fasteners before the testing procedure was started. All fastener threads were sprayed with dry molybdenum disulfide lubricant and allowed to dry before testing took place for repeatable results. The 1/4" tapped hole in the bottom test fixture was

also sprayed with the dry moly lube before testing took place and again half way through testing procedures and allowed to dry before continuing.

Testing speed is in accordance to ASTM E8M-01 Section 7.6.3.2. For a 1/4" bolt, two kips per minute comes in right in between the specifications range of 10,000 to 100,000 psi per minute of loading. The OMB-DAQ56 data recorder was set to its maximum rate of 4.6 Hertz and provided adequate frequency for data collection points. This produced at least 620 data points per test which lasted 130 seconds or longer.



Figure 7: Custom Test Fixtures, Gripper, Washer, and Fasteners

## CHAPTER 4: RESULTS

### 4.1 Fastener Strength

A total of twenty-four specimens were tested, twelve titanium 6-4 and twelve A286. Twelve test specimens each was decided upon after analysis based on the Choice of Sample Size section in Montgomery's book [27]. The calculation to arrive at this sample size is in Appendix B. The plots below are of the load vs. displacement data from all tests conducted.

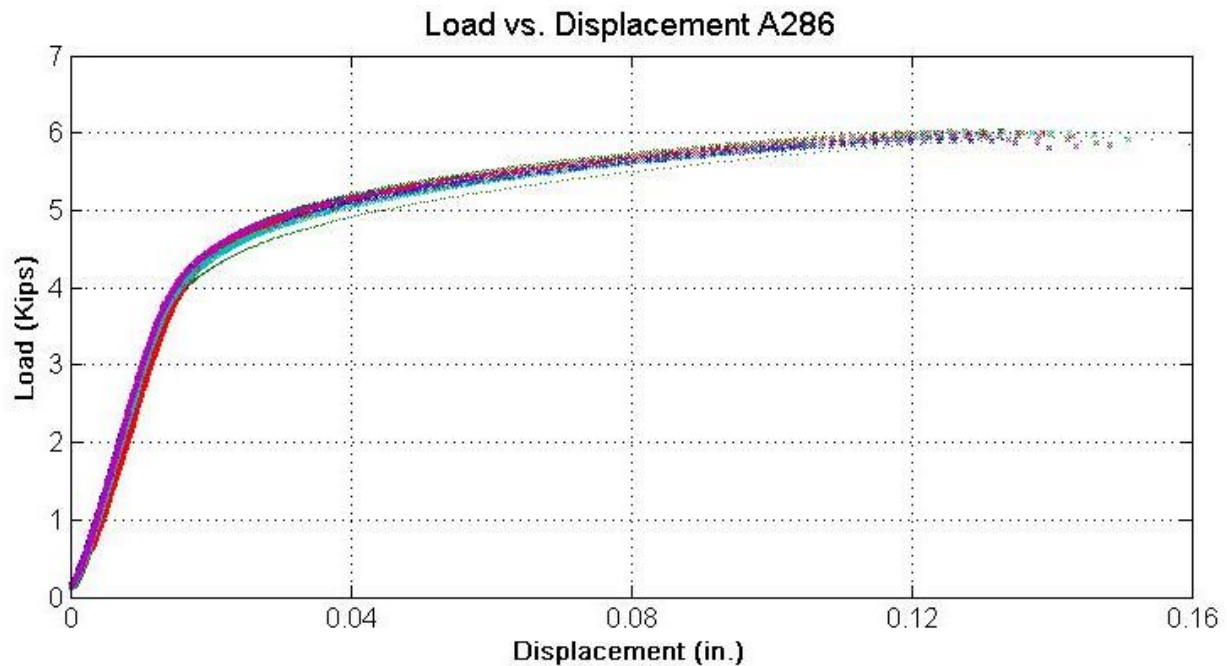


Figure 8: A286 Load vs. Displacement Tests

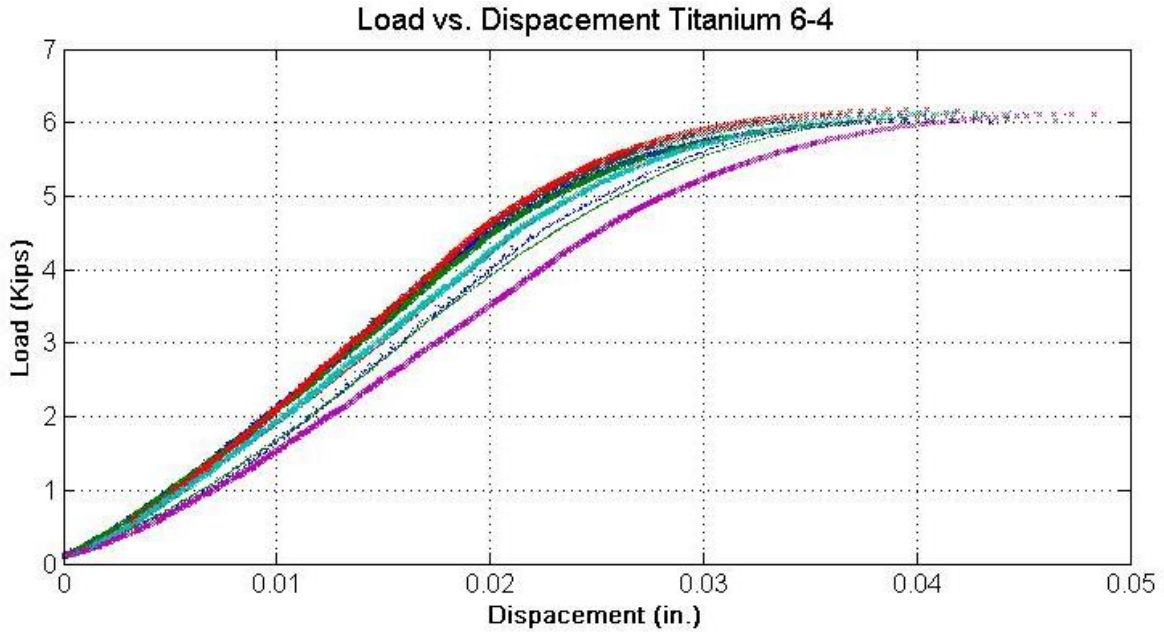


Figure 9: Titanium 6Al-4V Load vs. Displacement Tests

Note, it is very important to realize the different displacement scales from Figure 8 and 9. A representative graph in Figure 10 shows the two materials on the same plot to show a more accurate difference in displacement. The last point of each graph is where the specimen fractures.

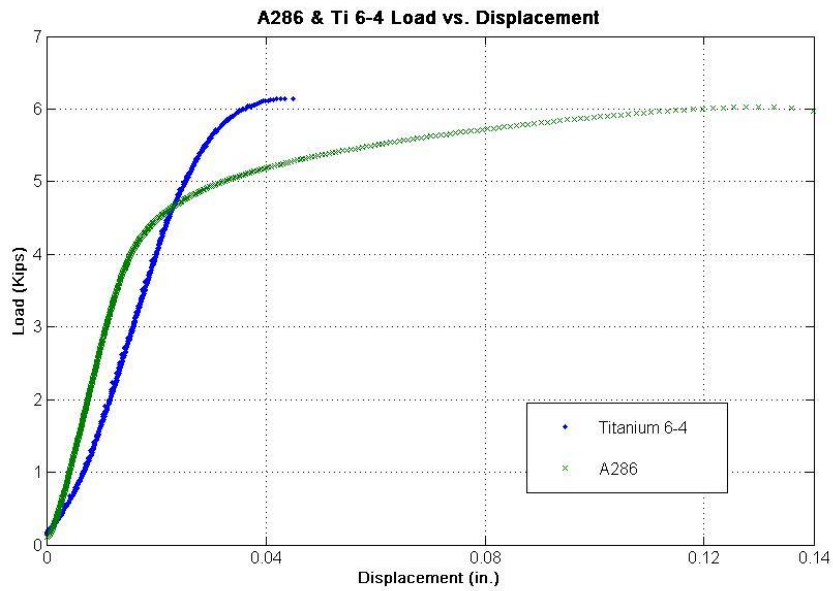


Figure 10: A286 & Titanium 6Al-4V Load vs. Displacement

Presented in Figure 11 is a box plot of the two materials yield strengths showing median, 25<sup>th</sup> and 75<sup>th</sup> quartiles along with minimum and maximums over the 24 total runs. Then Table 3 contains the average yield strengths and max tensile strengths.

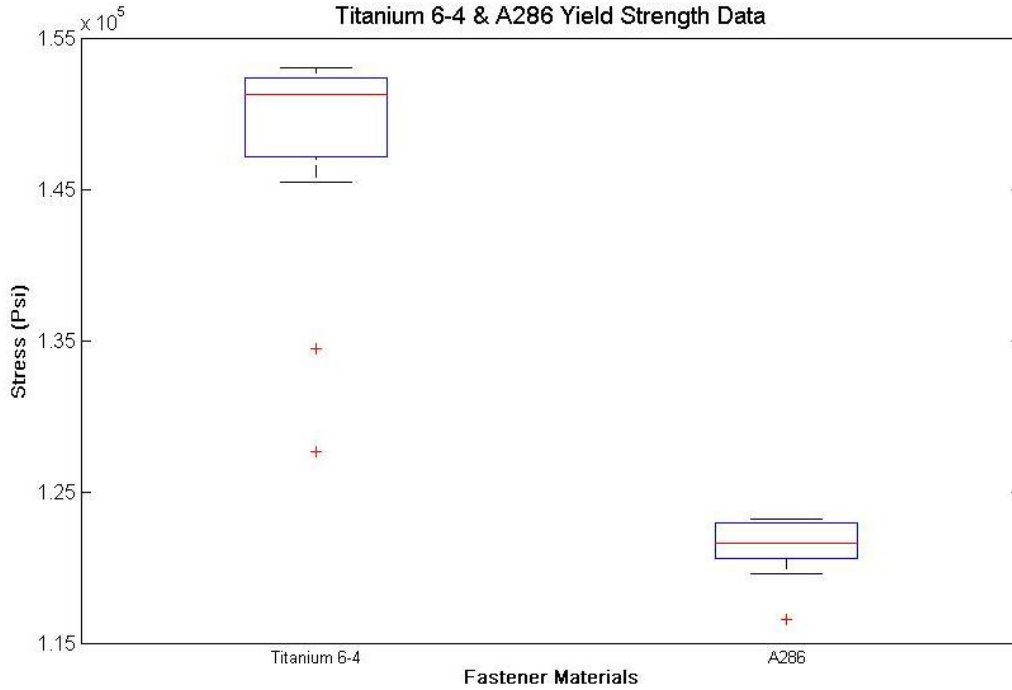


Figure 11: Yield Strengths for Titanium 6Al-4V and A286

As can be seen in Figure 11, the A286 has a much tighter grouping of yield strength data than the titanium 6-4. This can be seen graphically between Figure 8 & 9. The data points are much tighter throughout the whole test range for the A286.

Table 3- Fastener Yield Strengths

Material:	Yield Strength (psi)	Tensile Strength (psi)
Titanium 6Al – 4V Average	147,646	167,929

Table 3 (Continued)

<b>Minimum</b>	127,633	165,785
<b>25<sup>th</sup> Quartile</b>	148,018	169,900
<b>75<sup>th</sup> Quartile</b>	152,195	168,941
<b>Maximum</b>	153,136	169,787
<b>A286 Average</b>	121,349	164,219
<b>Minimum</b>	116,534	162,251
<b>25<sup>th</sup> Quartile</b>	120,642	163,371
<b>75<sup>th</sup> Quartile</b>	122,865	165,152
<b>Maximum</b>	123,196	165,913

The average maximum tensile load for A286 is 5,977 pounds while the average maximum tensile load for the titanium alloy is slightly higher at 6,112 pounds. This goes to show that these two materials are very closely matched for ultimate tensile strength and is why they are being compared in this study. The real question we are after however is how much displacement these fasteners can withstand when going from yield to fracture.

#### 4.2 Ductility Index

For these characteristics the ductility index will be calculated. The ductility index definition used in this thesis is pulled from Appendix A.5 of NASA Standard 5020. “The ductility is quantified by the ratio of plastic deformation at rupture to elastic deformation at rupture.”[7]. Figure 12 is a plot of load vs. displacement for A286 explaining graphically how the ductility index is calculated followed by table 4 which contains ductility indexes for A286 and Ti 6-4.

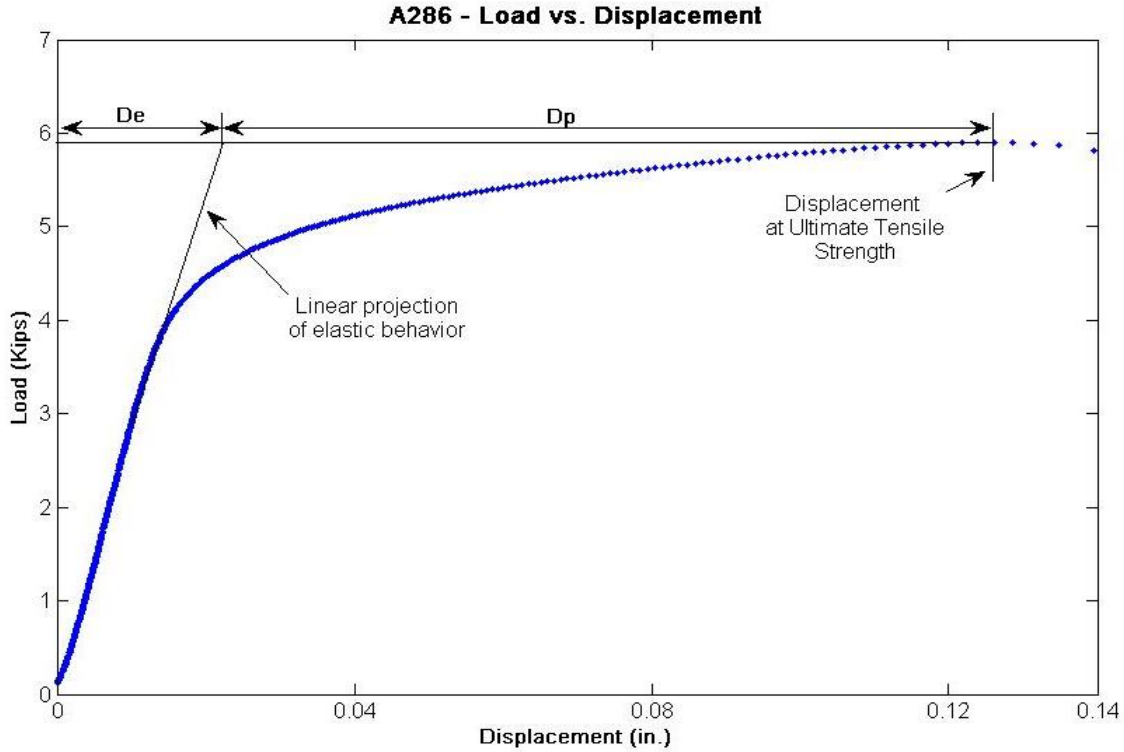


Figure 12: Ductility Index Quantification

In Figure 12 above,  $D_e$  stands for elastic displacement and  $D_p$  stands for plastic displacement. This ratio of  $D_p/D_e$  is the ductility index which will be referenced in this thesis. This will give a good indication as to the ductility in these two material fasteners. Ductility index is used because these are full scale fasteners and are not machined tensile test specimens. The test data for all 24 specimens with ductility index ratios are in Appendix C.

Table 4- Average Ductility Index

Material:	A286	Ti 6-4
Ductility Index Averages	5.40	0.53
Minimum	5.05	0.43
25 <sup>th</sup> Quartile	5.12	0.51



Table 4 (Continued)

<b>75<sup>th</sup> Quartile</b>	5.65	0.56
<b>Maximum</b>	5.90	0.59



Figure 13: Titanium 6-4 Fastener Failure



Figure 14: A286 Fastener Failure

The final note to take from the testing is the manner in which each material fractured. This can tell about the relative ductility of each of the materials. If a material being pulled in tension fractures perpendicular to the axis of loading force the material is considered more brittle. The opposite is true for failure of more ductile materials. A 45 degree fracture plane is expected from ductile materials when being pulled in tension. Figure 13 above is the titanium 6-4 specimen after failure occurred. Figure 14 is A286 after the specimen broke in testing. As these figures depict the titanium alloy fractures across only one thread which is perpendicular to the tensile loading. The A286 on the other hand fractures across three or four threads which is much closer to a 45 degree angle. These characteristics match the ductility indexes for the fasteners as well as fracture characteristics for brittle and ductile materials.

## CHAPTER 5: EXAMPLE PROBLEMS

### 5.1 Joint Design

When designing it is essential to choose fastener sizes and materials that will support the static and/or dynamic loads which the design will be subjected to in use. Physical quantities such as yield and tensile strengths along with ductility indexes are good general guidelines to know what might work but fasteners are used to hold joints together. Understanding bolted joints is essential to the design of fastener systems and aids in choosing the correct fasteners. Some simple joint diagrams can show loading scenarios to see how much force will be seen by the fastener and the joint while in use [22, 7, 28, 29].

Bolt diagrams are load vs. displacement graphs. The slopes of the lines are the spring constants of the bolt and joint material and the height is the applied preload to the bolt. The estimated external load for which the bolted joint will see in service is located by placing the upper end at the extension of the spring constant for the bolt and moving it until the bottom end contacts the spring constant line of the joint. Adding the external load in this manner reveals how much additional force and displacement the bolt experiences, as well as how much relief the joint experiences as shown, and explained in more detail, later in Figure 18. Calculations of these spring constants are gone over in the Meyer's paper [26] for the bolt as well as the joint. A basic joint diagram is in Figure 15 with an applied external load.

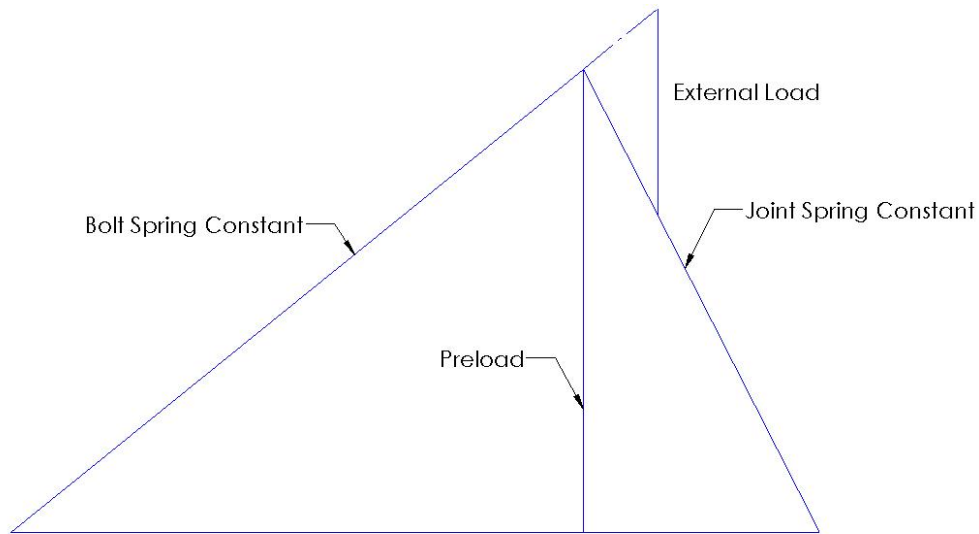


Figure 15: Joint Diagram with Applied External Load

The next important characteristic of joint design to look at are the effects of loading planes. Figure 16 shows physically what these loading planes are. A loading plane of one ( $n=1$ ) is considered worst case and is if the external load is applied right under the bolt head and the nut. The half loading plane ( $n=0.5$ ) is what will be used in the joint design examples to follow. A loading plane of zero ( $n=0$ ) would locate the load at the joint interface (not shown in figure). As the slanted lines show, the clamped part is reduced from the whole joint when  $n=1$  to half and is why the amount of displacement from the vertical preload line to the dashed line in Figure 17 is smaller with the half loading plane.

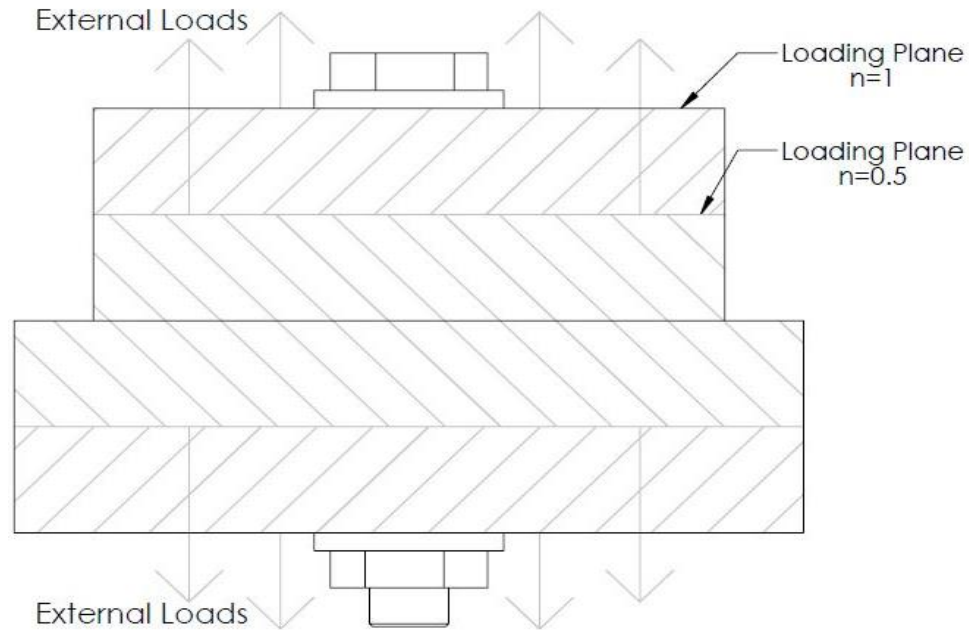


Figure 16: Bolted Joint with Loading Planes

These loading planes distinguish between the clamped and clamping parts of the joint and therefore change the bolt diagram's displacement axis (x-axis). For the following examples a half loading plane will be used since that is reasonable to assume since it represents most joints better than the other extremes. A worst-case scenario of loading planes, below the head and nut, will also be presented in this chapter to see how much of an effect these planes have on the loads seen by the bolt. A joint diagram showing this effect of loading planes is shown in Figure 17. The solid line represents the original scenario with loading planes right under the head and nut. The dashed line is the half loading plane scenario. Note the change in where the dashed line moves along the x-axis compared to where the solid line was. The clamped part (the joint) is now smaller with the half loading planes. This also changes the relative spring constants for the bolt and joint as can be seen by the slopes of the lines.

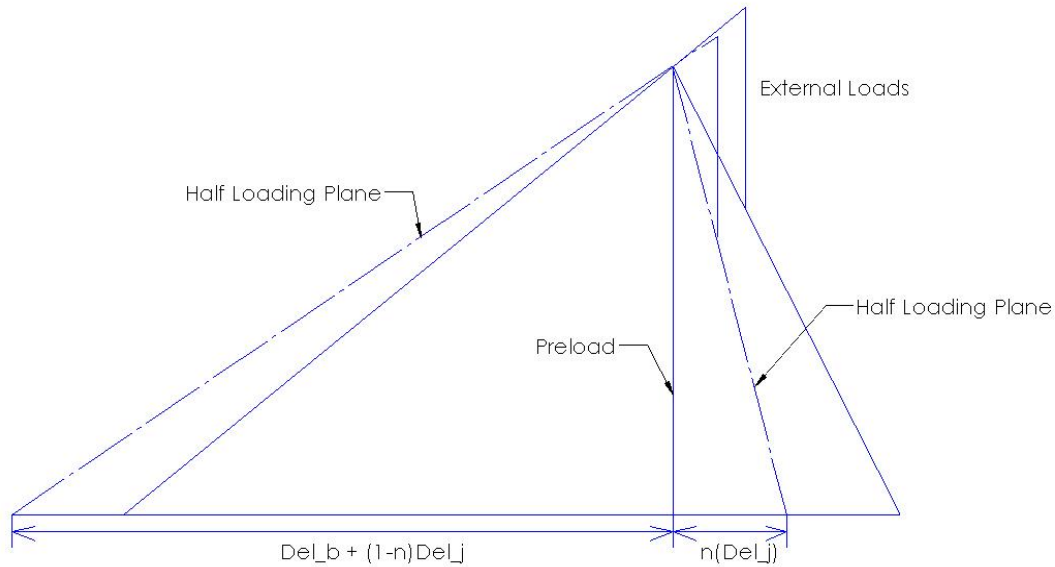


Figure 17: Joint Diagram Loading Plane Effects

The final consideration that needs to be taken into account for the joint diagrams are the uncertainties in the relationship between applied torque and the actual preload that it puts on the bolt. These papers [7, 28] state that it is a safe estimate to assume a preload uncertainty of plus or minus 25% for hand-operated torque wrenches during application and will be used in the following scenarios. If the bolt is instrumented however this can be reasonably taken down to plus or minus 5%. The torque tension values will not be discussed in this thesis, as it is a lengthy discussion so these uncertainty percentages will be used. Torque-tension guidelines are gone over in NASA Standard 5020 Section 5.8 [7].

A value that will be held constant for the joint design examples is the joint length. Each bolt is 2 inches so a joint length of 1.425 inches will be used. This is taking into account two washers with a nominal thickness of 0.06 inches, a nut with thickness of 0.375 inches and 0.08 inches of thread exposed to ensure full thread engagement as stated in NASA 5020 Section 5.6.1 [7].

## 5.2 Bolted Joint Diagram Values

The first step in making a joint diagram is calculating the spring constants for the load vs. displacement graph. This spring value for the bolt can be found using a modified Hooke's Law equation found in the Meyer's paper [22]. This equation is fully explained in Appendix D along with the calculation for A286.

To find the spring constant in the joint is a more complex problem. For the following joint diagram examples the third joint area equation presented in Meyer's paper is used. This area is for if the diameter of the joint is equal to or greater than three times the area of the washer in the joint. The other two areas present in Meyer's paper are a sleeve and an area that would be in between the sleeve and area used in the joint diagram examples in this thesis. The equation for area used is thought to be for the most general application but all three will give similar results though the area used is the most conservative since it's the largest area.

The final variable that needs to be addressed is the applied external load to the joint diagram examples. The Meyer's paper [22] states for good joint design to choose a preload force that is at least twice as much as the external force that the joint will experience in use. Therefore, for these joint design examples the preload will be specified based on minimum yield strength of data collected in this research then the example's external loads will be applied based on preload. This loading will keep the relationship between the bolt and joint linear since investigations have shown that the lower portion of the joint spring constant is actually non-linear for compressed parts [22].

Minimum yields from the test data in Table 3 collected in this research will be used to calculate preloads in accordance to VDI 2230 [39]. The necessary data for the joint diagram examples are in Table 5.

Table 5- Preload Scenario Loadings

<b>Materials:</b>	<b>Titanium 6-4</b>	<b>A286</b>
<b>Minimum Yield Load</b>	4,643 lb	4,238 lb
<b>90% Preload</b>	4,179 lb	3,815 lb
<b>65% Preload</b>	3,018 lb	2,755 lb
<b>Young's Modulus</b>	12,931 ksi	16,990 ksi
<b>Spring Constants</b>	280,000 $lb/in.$	363,000 $lb/in.$

### 5.3 Constructing a Joint Design Example

A joint diagram example consists of six points connected by lines. The points were labeled A through F for organization. Point A is at the origin and connects to B, the slope of which represents the tensile spring constant of the bolt. Point B connects straight down to C which represents the preload on the bolt. Point B also connects to point D which represent the compressive spring constant of the joint. In good design, the joint should be stiffer than the bolt as shown in Figure 18. Point E connects to F in a vertical line representing the external load that is applied to the joint. The top of this external loading line, point E, lies on the extension of the bolt spring constant line and is moved up or down until the bottom of the line, point F, contacts the joint spring constant line. Shown in Figure 18 are the locations of these points in a joint diagram. The steps needed to find these points are given in Appendix E.

Basically, the preload is calculated based on the minimum yield of the test data collected. This sets the height of line BC. The external load, line EF, is then calculated from that preload by dividing by 2 as explained in Section 5.2. The slopes of the line determine where on the graph's x-axis line BC and EF will be located. Depending on the assumed loading planes for each joint diagram example the locations will be adjusted.



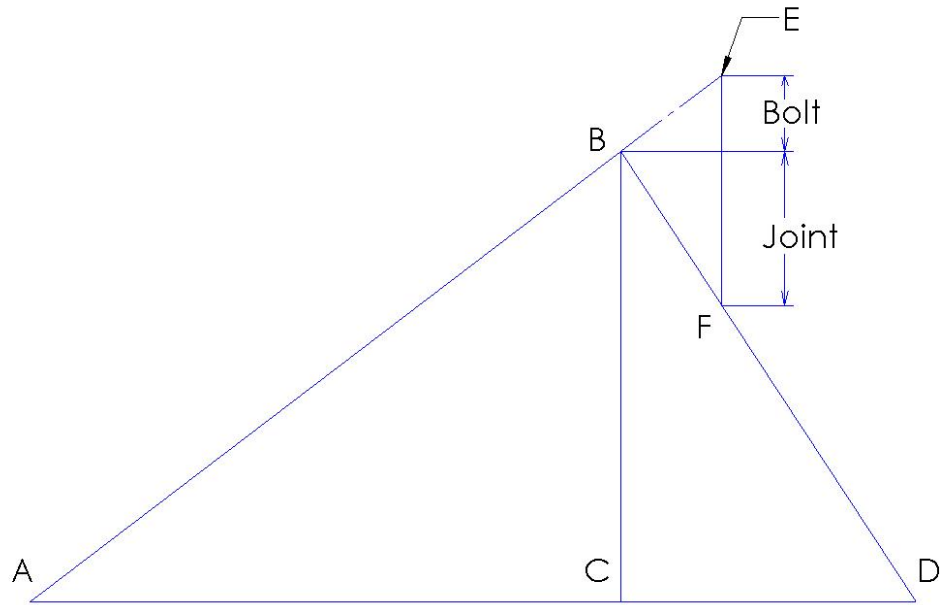


Figure 18: Joint Diagram Naming Convention

#### 5.4 Interpreting a Joint Design Example

The points on the graph represent important aspects of the joint's loading. The y-coordinate of Point B is the preload that the bolt is tightened to. The y-coordinate of Point E is the max load seen by the bolt and is the most important point to be taken from the graph. This point is needed to make sure that the bolt will not fail while it is in use. The interesting thing that the joint diagram does however is it shows how much of the external load the bolt is taking up and how much the joint is taking. Note the horizontal line that is drawn to the right from Point B to the external load line, from that horizontal line to point E is the amount of external load the bolt is taking. From that horizontal line down to Point F is how much the joint is taking. As can be seen from Figure 18, the joint takes more of the external load than the bolt. This is how a properly designed joint should function.

The amount of external load that the bolt sees can be adjusted through proper design. Meyer's paper [22] has shown that a more springy bolt and stiffer joint is a better design. The

more elastic the bolt, the lower the slope of the line. The shallower this line becomes, the less distance between Point E and a line drawn horizontally to the right of Point B. This means that the bolt sees less load if the slope of the joint line is relatively steep. The loading planes also come into play with this calculation. The farther the loading planes are from right under the head and nut ( $n=1$ ) the steeper the joint line becomes and the shallower the bolt line becomes.

Another important location to take note of is the x-coordinate of Point D. If the external load grows above the designed value the joint will separate at this point. Once the external load grows or the bolt elongates past that x-coordinate of Point D, the joint will separate and the bolt will now experience the full tensile load that is being applied. In some cases however, the bolt may rupture before separation of the joint occurs. To figure this out consult Section 5.5.

### 5.5 Using the Joint Diagram

As stated in the Section 5.4 the y-coordinate of Point E in Figure 18 is the maximum load seen by the bolt with the external load applied. This is the important value in determining if the fastener will fail in service. There are two ways for failure to occur. The bolt may rupture before joint separation or the joint may separate. Joint separation occurring sometimes is considered a failure and even if not, the bolt will experience the full load at separation. An easy way to figure out which will occur first, rupture or separation, NASA Standard 5020 can be consulted. Figure 5 of the 5020 Standard, shown below as Figure 19, is a flow chart to determine if separation or rupture will occur first. Seen in the figure, the Section the flow chart refers to (Section 6.2.1.1 and 6.2.1.2 in Reference [7]) are Margin of Safety calculations based on if rupture or separation occurs first. The Figure 6 referred to at the bottom of the flow chart is a graph in NASA Standard 5020 explaining the same thing Figure 12 from Chapter 4 of this thesis does which shows how to calculate  $\delta_p$  and  $\delta_s$ .

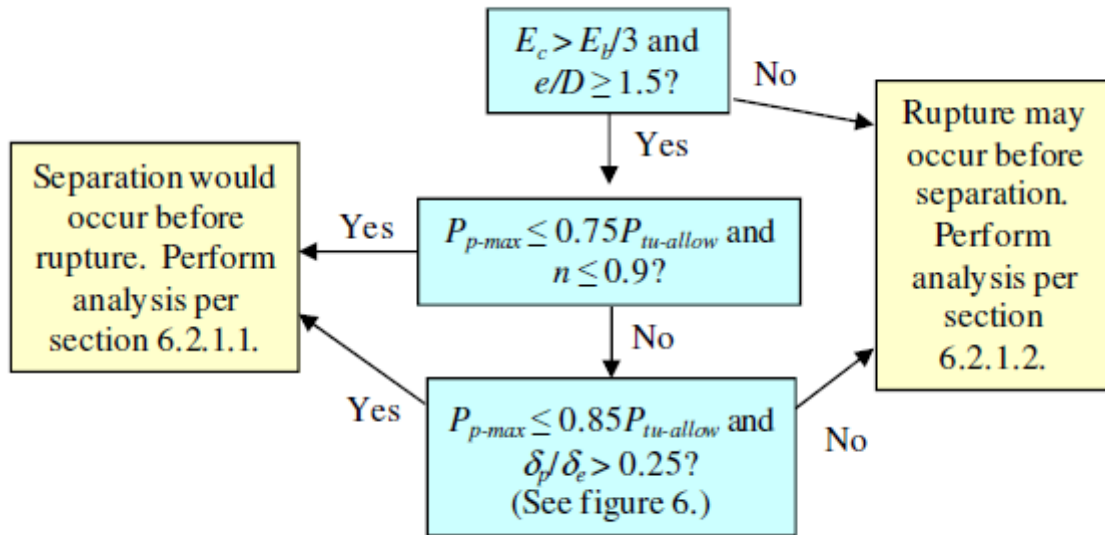


Figure 19: NASA 5020 Joint Separation Flow Chart [7]

In this flow chart,  $E_c$  is the elastic modulus of the clamped material and  $E_b$  is the elastic modulus of the bolt.  $D$  is the diameter of the head of the bolt or washer and  $e$  is the length to the closest part from the bolt measuring from the center of the bolt to the next part.  $P_{p-max}$  is the maximum preload on the bolt and  $P_{tu-allow}$  is the allowable ultimate tensile strength for the material. Also in the second step is  $n$  which is the loading plane. A value of 1 is for full loading planes under the head of the bolt and nut and 0 would be if the joint was being pulled from the middle of the two clamped parts. The final two values are  $\delta_p$  and  $\delta_e$ , which are the displacements at the end of the plastic and elastic regions. These are the values that are pulled from the ductility index graphs shown in Appendix C and summarized in Table 4 of Chapter 4.

The elastic modulus values are pulled from stress-strain graphs that are calculated from the load vs. displacement data collected in testing and seen in Table 5.  $E_c$  is chosen to be an aluminum alloy with modulus of 10,000 ksi. The  $e$  value was chosen in the joint diagram examples so that it would meet the requirement to move onto the next step down in the flow

chart. It is 0.75 in. which is reasonable for a general-purpose joint example.  $P_{p-max}$  is the preload for each joint design example and  $P_{tu-allow}$  is the minimum tensile strength for the materials from the data collected for this thesis. As stated previously  $\delta_p$  and  $\delta_s$  are pulled from Table 4 of this thesis and were calculated based off the load vs. displacement graphs of the data collected for this thesis.

In the joint diagram examples to follow, a flat safety factor of 1.4 was placed on the maximum load to be seen by the bolt. If the flow chart in Figure 19 shows that the joint would separate before rupture than the load at separation is calculated and the safety factor was placed on that value. The value with the safety margin is then compared to the minimum tensile strength of the data collected to see how the fasteners would perform if the full tensile load is seen by the bolt upon joint separation.

## 5.6 Joint Diagram Examples

A total of 18 joint diagram examples were calculated to see how these two materials would respond in different preload and external loading scenarios. These 18 examples come from three basic configurations: 90% preload with half loading planes, 65% preload with half loading planes and 65% preload with full loading planes. From these three configurations torque-preload uncertainty percentages of plus or minus 25% were added as discussed in Section 5.1. Table 6 shows all the joint design examples calculated. The rest of this Chapter looks more closely into the interesting aspects of some of these examples. The ones not discussed in detail are in Appendix F which are marked with \*\* in Table 6.

Table 6 - Joint Diagram Examples

<p><b>Half Loading Planes</b> (Titanium 6-4 and A286)</p>	115% (90% +25% Uncertainty)
	90% (Nominal Case)
	65% (90%-25% Uncertainty)**
	90% (65%+25% Uncertainty)**
	65% (Nominal Case)
	40% (65% - 25% Uncertainty)**
<p><b>Full Loading Planes</b> (Titanium 6-4 and A286)</p>	90% (65% +25% Uncertainty)
	65% (Nominal Case)
	40% (65%-25% Uncertainty)**

### 5.7 90% Yield Preload with +/- 25% Uncertainty from Torque

The first joint diagram example that will be investigated is a comparison of titanium 6-4 and A286 based on an applied preload of 90% of each materials minimum yield strength from the data which was collected. This percentage is pulled from Section 4.2 of VDI 2230 [29] as a value most frequently applied. Some standards take the bolts up to 100% of minimum yield strength but with the minimal strain hardening of the titanium alloy the calculations show that the bolt will fail while being installed, if the upper limit of 25% torque-preload uncertainty (115% Preload) is reached, which has happened previously [8,20,19]. The flow chart and safety margin calculations in Section 5.5 will be discussed after each joint diagram example graph is presented in this section. This chapter is meant to show scenarios where the titanium alloy would not be suitable to use instead of A286 as well as where the titanium alloy can be used safely in place of A286.

### 5.7.1 115% Preload with A286

This first example shows the upper uncertainty range of A286 with an applied external load equal to half of the 90% Preload. This will be 115% (90% preload +25% uncertainty) preload of the minimum yield of the specimens tested.

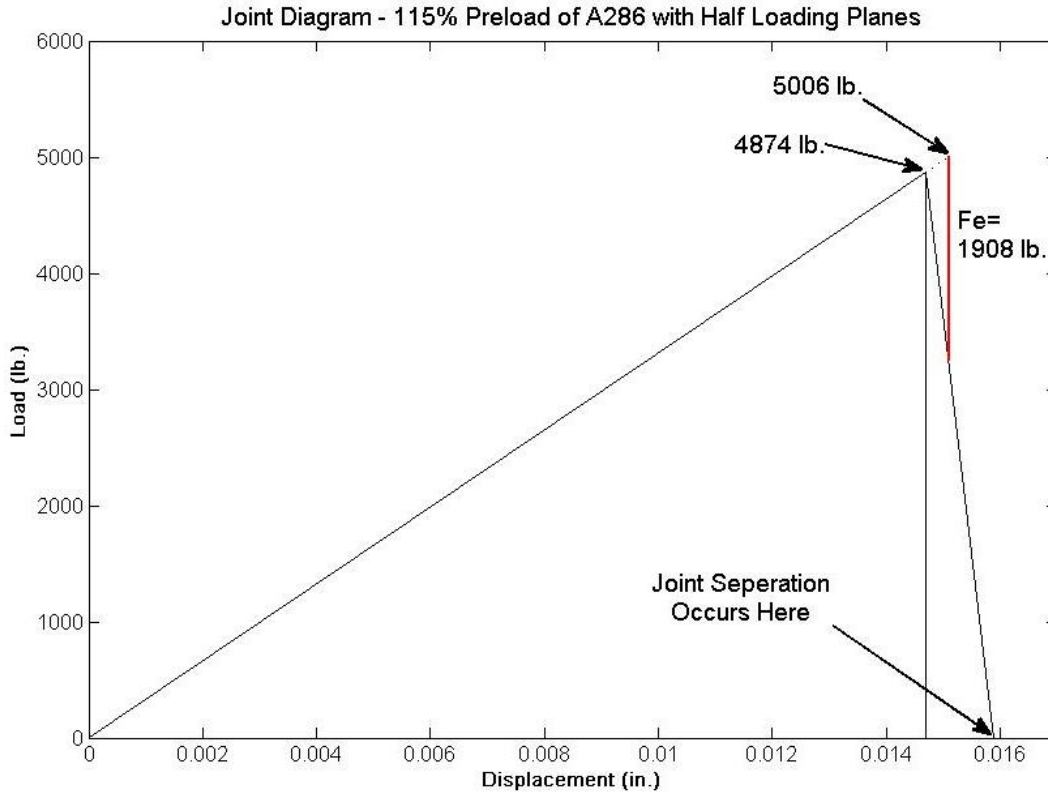


Figure 20: 115% Preload of A286 Joint Diagram

Using the flow chart in Figure 19 from NASA STD-5020 it can be determined if a joint will rupture before separation or separate before rupture. This chart was followed and A286 in this loading scenario will separate before rupture of the fastener as expected because of the high ductility index. As explained in Section 5.4, joint separation will occur when the bottom of the external load line ( $F_e$ ) reaches the x-axis. At this point none of the load is carried by the joint and the bolt will see the entire tensile load that is being applied. In this joint diagram example the

load at joint separation will be 5,772 lb. Multiplying this by a safety factor of 1.4 give a value of 8,080 lb. which is above the 5,906 lb. minimum tensile strength of the A286 fasteners tested for this thesis. A286 in this loading example will not break upon joint separation. However, with a 40% safety margin it will not be acceptable to use.

### 5.7.2 115% Preload with Titanium 6-4

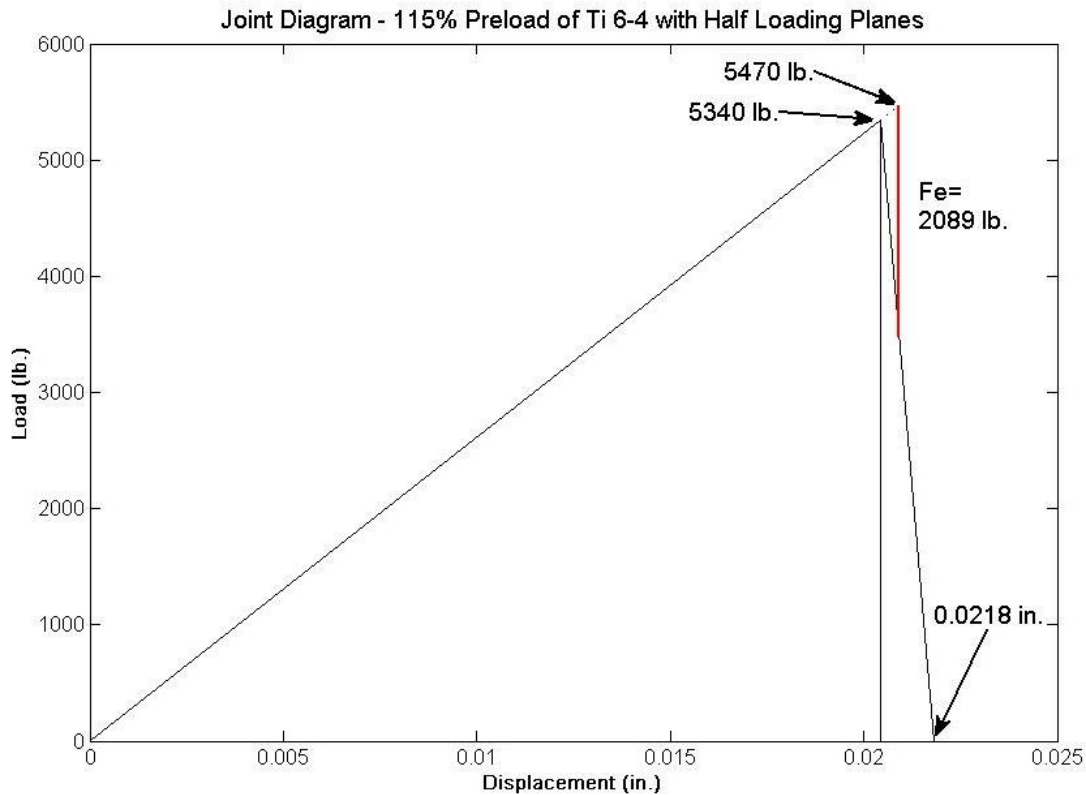


Figure 21: 115% Preload of Titanium 6-4 Joint Diagram

Going through the same flow chart as the previous example, the flow chart shows that titanium 6-4 may rupture before separation occurs in this joint diagram example as to be expected due to the much lower ductility index compared to A286. This is an example where the titanium alloy would fail during use and A286 would not. At a load of 5,470 lb. the titanium would be out of the linear-elastic range of its load curve and displacement will pick up faster than load since it will be in the plastic deformation region.

Calculating the load at separation for this joint diagram example the bolt will fail before the joint separates. The joint will be totally unloaded at 0.0218 inches which can be seen in Figure 21. At this point the bolt will be seeing the full external load which will be 6,104 lb. The minimum tensile strength for the experiments conducted for titanium 6-4 alloy was 6,035 lb. This means that the bolt will break before the joint separates for this minimum case. The flow chart from NASA 5020 works as designed and the bolt would rupture due to external loads before the joint separates.

### 5.7.3 90% Preload with A286

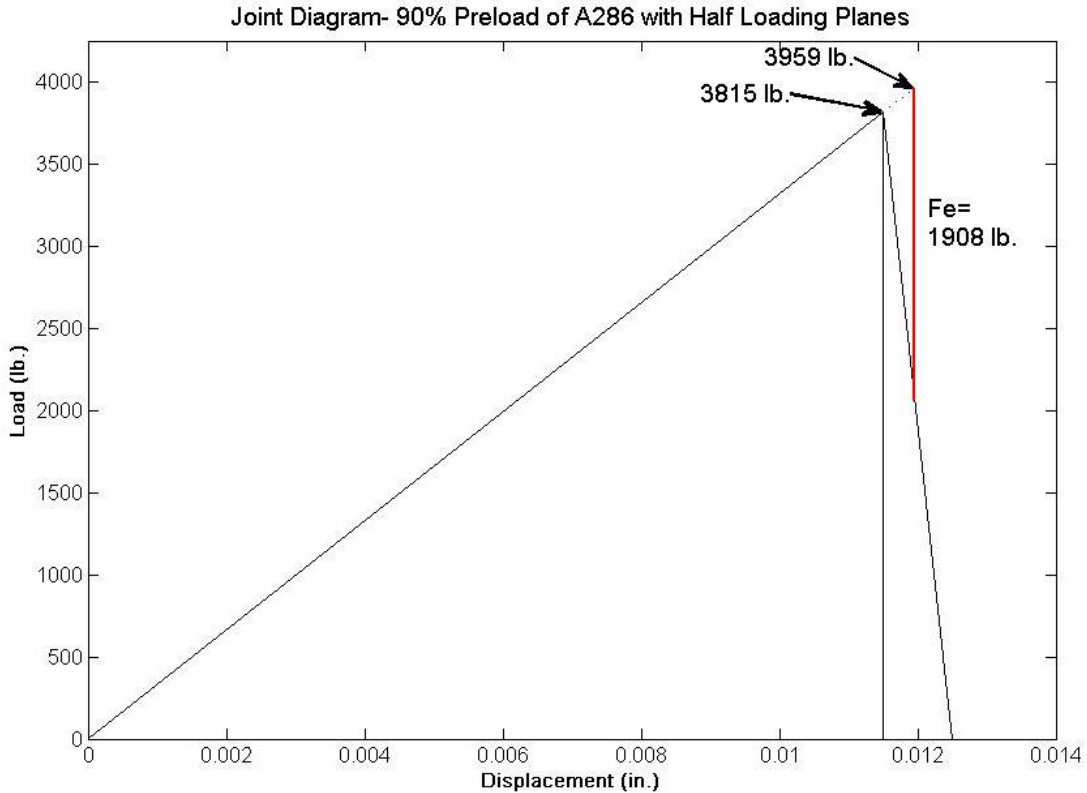


Figure 22: 90% Preload of A286 Joint Diagram

The 90% joint diagram example will separate before rupture occurs for A286 since the same occurred for the 115% case. The load seen by the bolt once the joint separates is 4,538 lb. With a flat safety margin of 1.4 that takes the load to 6,353 lb. The tensile strength for the



minimum A286 test was 5,906 lb. This means that the A286 should not be used if preload is taken to 90% of minimum yield strength and the loading planes are assumed to be half if a safety factor of 40% is warranted. However, the fastener will not break at separation. If the safety factor is brought down to 1.2 for this case the safe load would be 5,446 lb. which would be considered safe to use.

#### 5.7.4 90% Preload with Titanium 6-4

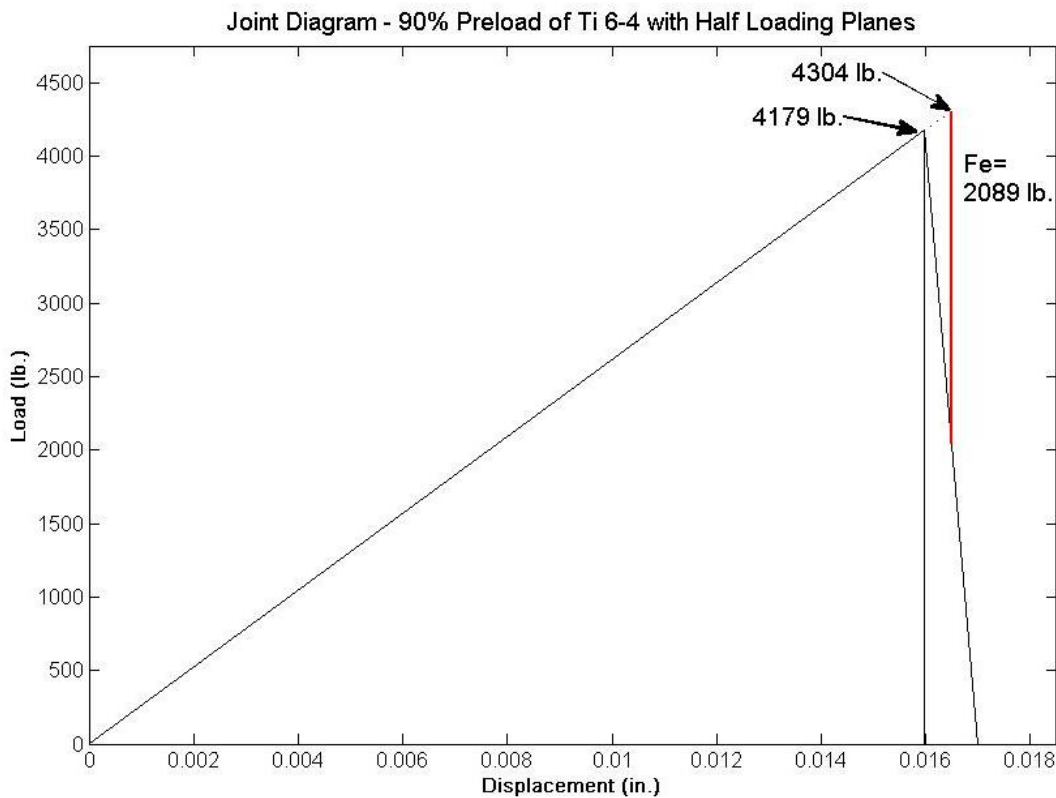


Figure 23: 90% Preload of Titanium 6-4 Joint Diagram

Following the flow chart in Figure 19 the titanium 6-4 with 90% preload the joint will now separate before rupture which differs from the 115% case previously viewed. The load seen by the bolt once the joint separates will be 4760 lb. With the same flat safety factor of 1.4 this value is raised to 6,664 lb. The tensile strength of the minimum titanium 6-4 test is 6,035 lb. This means that with a preload of 90% and half loading planes the fastener will not fail in use but the

40% safety margin will not be met. Like the scenario in Section 5.7.3 if the safety margin is brought down to 1.2 this means the safe load would be 5,712 lb. which is below the tensile strength. This means this joint design example would be considered safe if only a 20% safety margin was necessary.

### **5.8 65% Yield Preload with +/- 25% Uncertainty from Torque**

The second main loading scenario that will be evaluated is a comparison of these two materials with a preload of 65% of their minimum yield strengths. This value was taken from the NASA Technical Memorandum [28] which states that an initial preload of 65% is specified for some NASA space flight hardware. These values were also taken from the minimums of the test to have consistency between joint diagram examples.

Since both materials did not meet margin tests at a nominal 90% preload, 65% will now be looked at to see which fasteners can be used at this nominal level and have acceptable margins. Since the 90% joint diagram examples presented above have a slightly higher external load but the margin was not met this section will not go deeper into the upper uncertainty level of 65% which would also be 90% (65% +25% Torque uncertainty) just with a slightly smaller applied external load. Again, the difference between the 90% nominal joint diagram example and a 90% example from an upper uncertainty example from 65% is the external load. Since the external load is calculated as half of the nominal preload the external loads applied to the joint diagram examples will be different. The examples presented below are of 65% nominal preload meaning the external load is half of the 65% minimum yield for the materials.

#### **5.8.1 65% Preload with A286**

In this joint diagram example a nominal case of 65% is calculated which means that there is no uncertainty in the torque-preload equivalence. Preload is again taken as 65% of the

minimum yield strength from the data collected in testing for this thesis which comes out to be 2,755 lb. The external load is then calculated as half of this value which is 1377 lb.

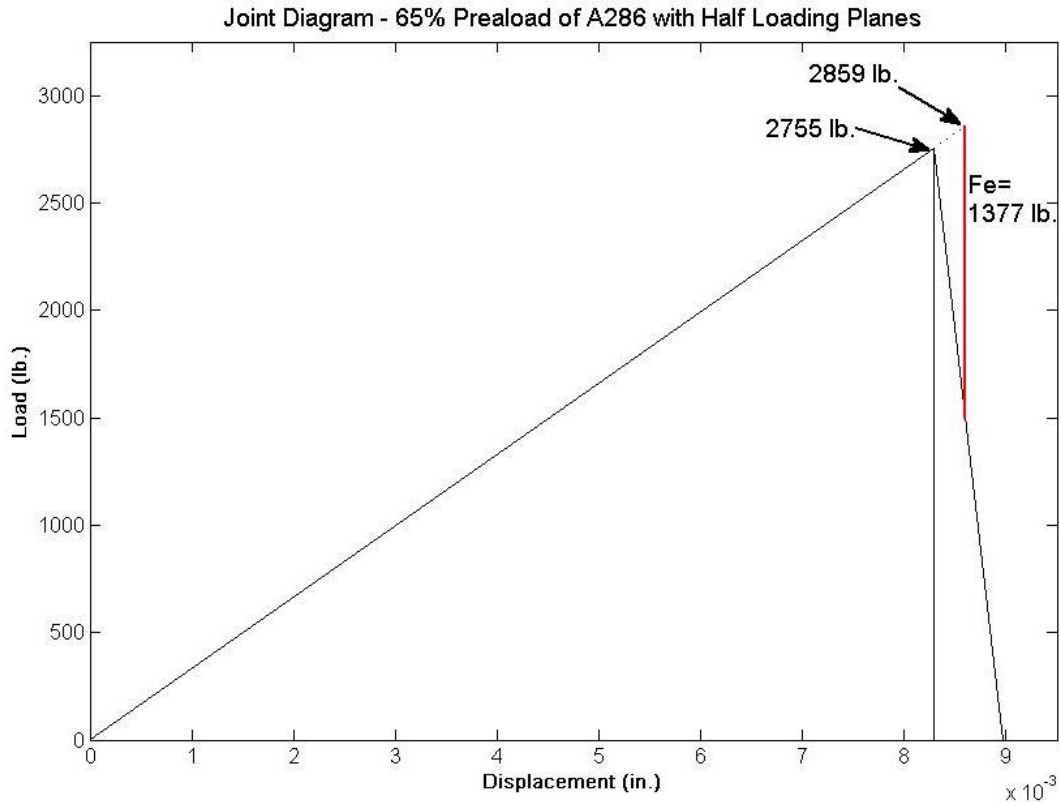


Figure 24: 65% Preload of A286 Joint Diagram

This joint will separate before rupture following the flow chart in Figure 19. At the point of joint separation the bolt will see the full amount of the tensile load which will be 3,256 lb. Again, multiplying this value by a safety factor of 1.4 it bring the load up to 4,560 lb. which is below the minimum tensile strength of the A286 bolts tested of 5,906lb. This means that A286 is safe to use at 65% preload in this joint diagram example.

### 5.8.2 65% Preload with Titanium 6-4

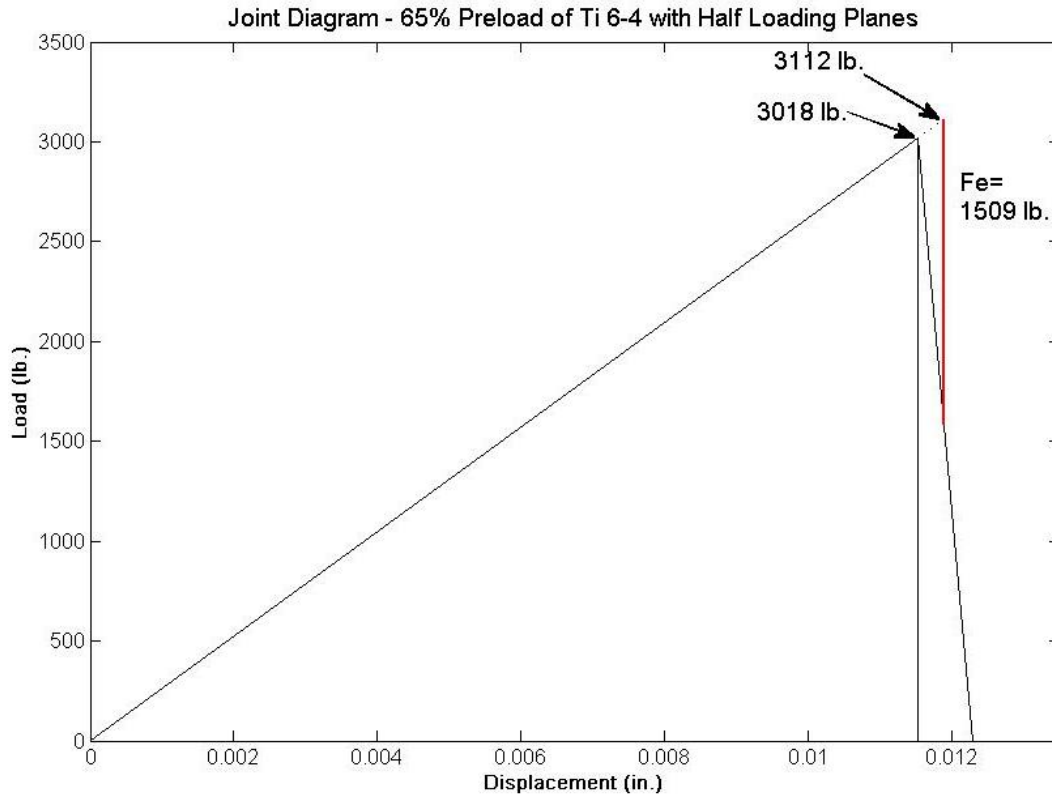


Figure 25: 65% Preload of Titanium 6-4 Joint Diagram

In this joint diagram example titanium 6-4 is preloaded to 65% of the minimum tensile strength seen in the testing conducted for this thesis. The joint will separate before rupture and at that point the bolt will see a load of 3,441 lb. Multiplying this by a safety factor of 1.4 gives a value of 4,818 lb. which comes in below the minimum tensile strength seen by the titanium 6-4 specimens in testing of 6,035 lb. This means titanium 6-4 can safely be used with 40% margin in this joint diagram example.

### 5.9 65% Yield Preload with +/- 25% Uncertainty from Torque and Full Loading Planes

Since it was shown in the first two examples of this Chapter the worst case of 90% loading will cause the titanium 6-4 to fail and A286 to not meet the safety margin in use with half loading planes the full loading planes it will assuredly break the fasteners. Because of this,

the worst case loading planes of nominal 65% preload joint diagram examples will be calculated to see how these fasteners will perform. This means the 90% (65% preload + 25% uncertainty) preload will be calculated with full loading planes first to take the upper uncertainty level.

### 5.9.1 90% Preload with A286 and Full Loading Planes

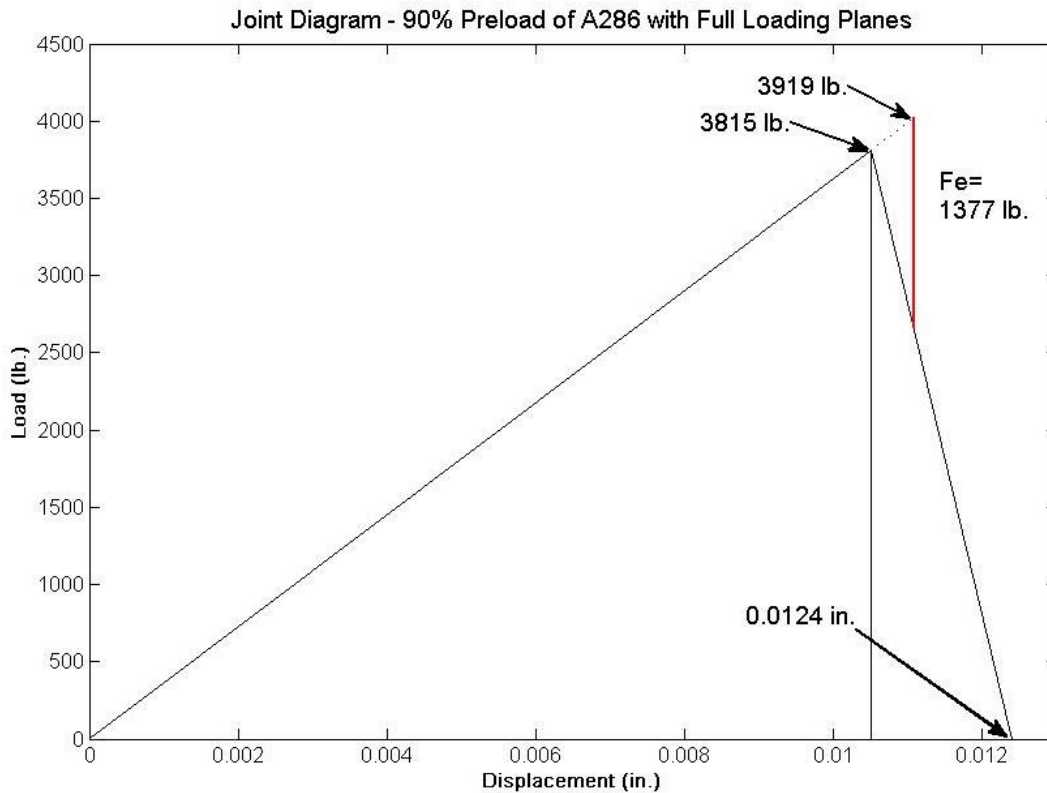


Figure 26: 90% Preload of A286 Joint Diagram – Full Load Planes

Figure 26 is the joint diagram example for the 90% preload (65% + 25% uncertainty) of A286 with full loading planes. The first thing to notice that has changed from the previous figures, with half loading planes, is the length of the joint compression and the slopes of the bolt and joint lines. The distance from the preload line to where the joint line hits the x-axis is now twice as long as the same preload example in Figure 22. The length of the joint diagram is still the same at 0.0124 in. but the amount taken up by the joint is now greater.

The joint will separate before rupture occurs and the load on the bolt when the joint separates will be 4,501 lb. With a safety factor of 1.4 that brings up the value to 6,301 lb. which is greater than the minimum tensile strength in the tests of 5,906 lb. This means that with full loading planes the A286 will not fail in use but it will not be able to function safely in this worse case loading plane example if 40% safety margins are needed. Like in Section 5.7.3 if the safety margin is brought down to 20% this joint diagram example will be deemed safe.

### 5.9.2 90% Preload with Titanium 6-4 and Full Loading Planes

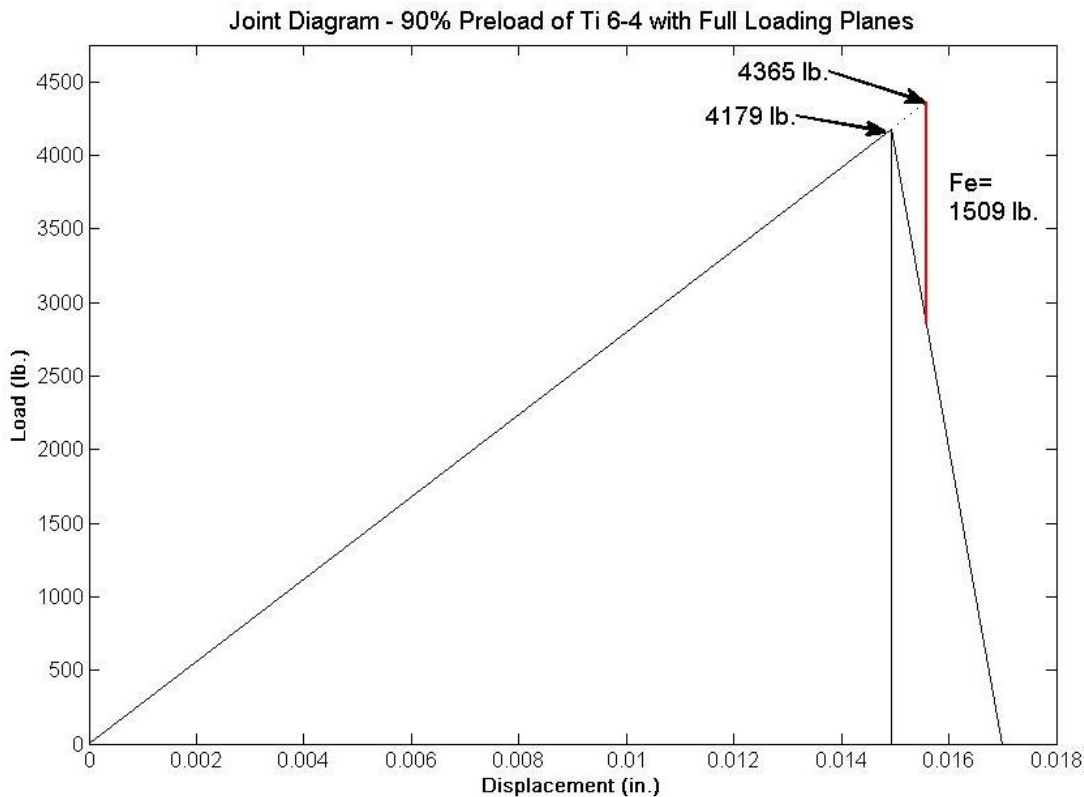


Figure 27: 90% Preload of Titanium 6-4 Joint Diagram – Full Load Planes

In the joint diagram example shown in Figure 27 the joint will separate before rupture of the fastener. When the joint fully unloads and the bolt sees the full tensile force being applied, the load will be 4,760 lb. Multiplying this by a safety factor of 1.4 give a load of 6,664 lb. The minimum tensile strength seen by the tests of the titanium 6-4 was 6,035 lb. This means that the

titanium 6-4 will not break when the joint unloads but the safety factor will not be met. Like in Section 5.7.4 if the safety margin is brought down to 20% this joint diagram example will be safe.

Since both the A286 and titanium 6-4 will not meet 40% safety margins for the upper limit of uncertainty in 65% preload assuming full loading planes the final two joint diagram examples will be shown. These will be the nominal 65% preload with full loading planes to see if they will pass safety margin calculations at joint separation.

### 5.9.3 65% Preload with A286 and Full Loading Planes

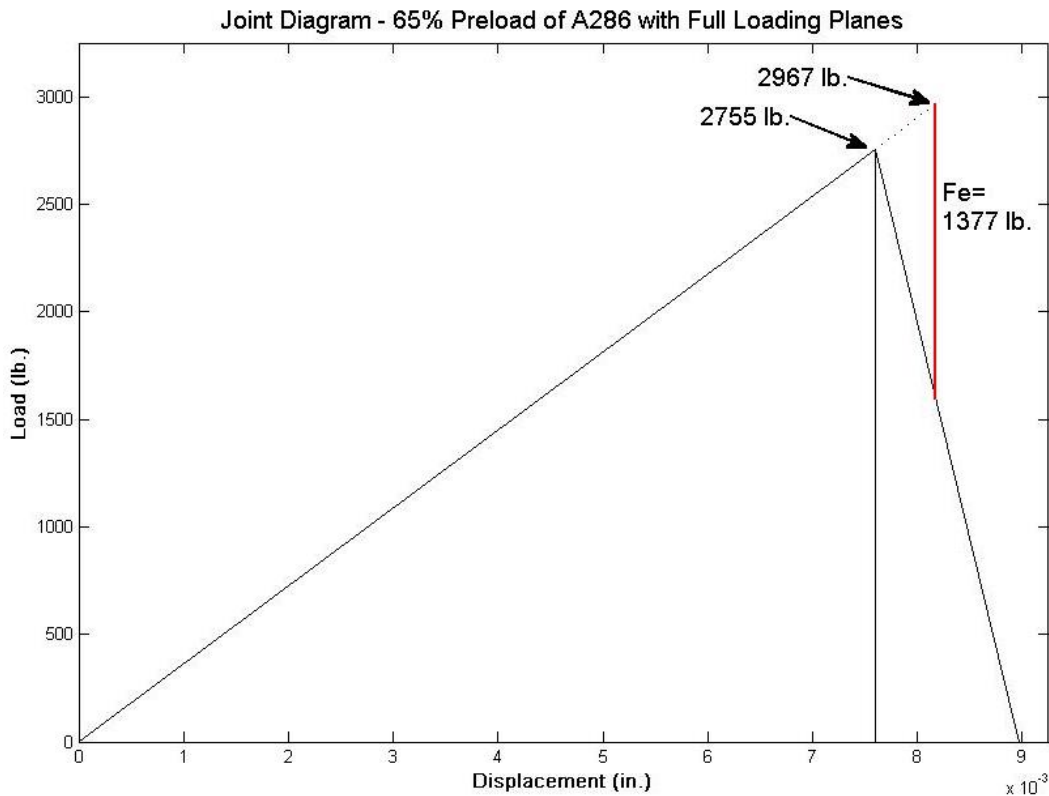


Figure 28: 65% Preload of A286 Joint Diagram – Full Load Planes

Figure 28 is the nominal case of 65% preload with no uncertainties in torque-preload equivalence. The joint will separate before rupture. At separation the bolt will see the full load of 3,256 lb. With a safety factor of 1.4 it brings the value to 4,559 lb. which is below the minimum

tensile load seen by the fasteners in testing of 5,906 lb. This means that this joint diagram example will pass with 40% safety margin when the joint is fully unloaded.

### 5.9.4 65% Preload with Titanium 6-4 and Full Loading Planes

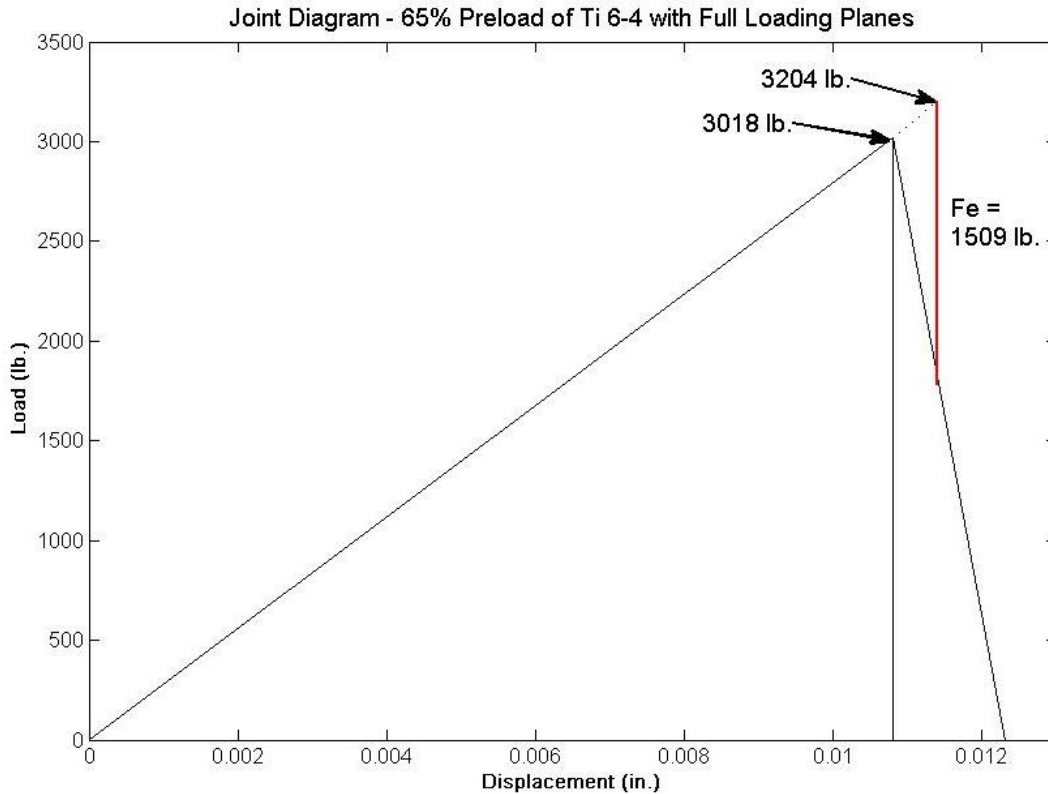


Figure 29: 65% Preload of Titanium 6-4 Joint Diagram – Full Load Planes

In this joint diagram example the nominal value of 65% is taken for preload assuming there are no uncertainties in the torque-tension equivalence. This joint will still separate before rupture with full loading planes and when the joint separates the bolt will see a load of 3,444 lb. Multiplying this by the safety factor of 1.4 will bring it to 4,821 lb. which is below the minimum tensile strength from the tests of 6,035 lb. This means that the titanium can be safely used at 65% preload with the assumption of full loading planes and 40% safety margins.



## CHAPTER 6: DISCUSSION

### 6.1 Tensile Test Data

This section of Chapter 6 will delve deeper into the test results presented in Section 4.1 which were yield and tensile strength data from the tests performed for this thesis. Figure 30 below is the same as Figure 10 and is a representative load vs. displacement graph of each material. The line with less displacement is the titanium 6-4 and the line with more is A286.

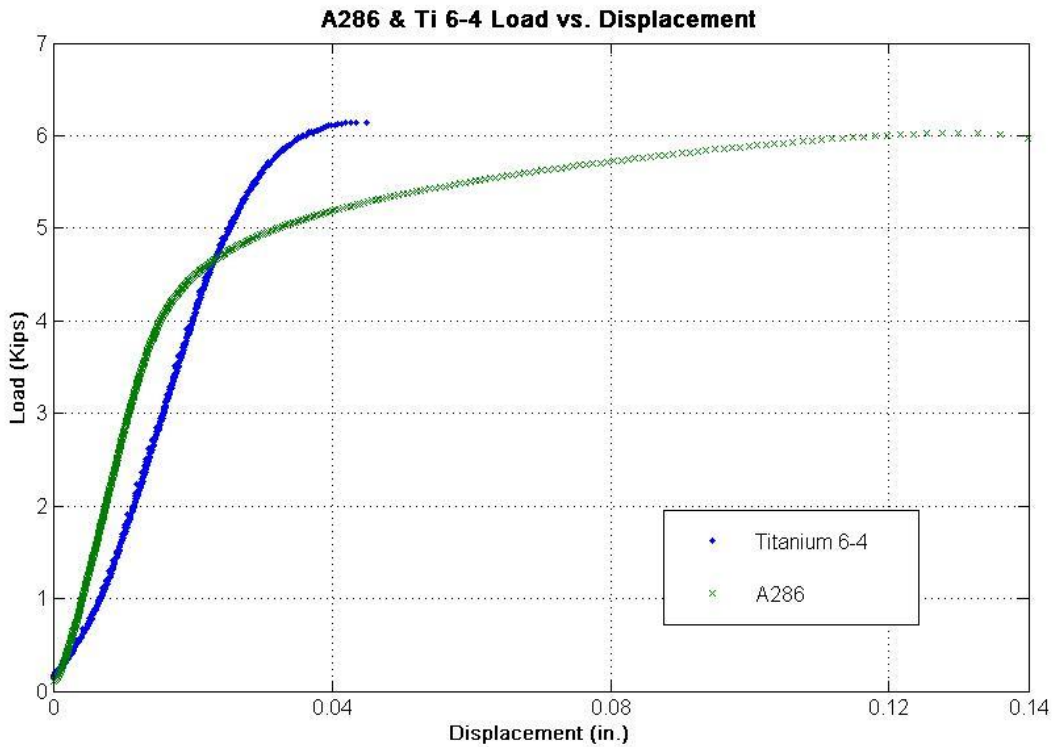


Figure 30: Representative Load vs. Displacement Graphs

From Figure 30 it can be seen that the tensile strengths of these two materials are very similar and the load they fracture at is close as well. The last point of each line is where the

specimens fractured in testing and each average was right around 6,000 lb. As the graph depicts however, the yield strengths differed more with the yield of titanium 6-4 being greater by over 26,000 psi, or 950 lb for these specimens. Overall however, these two materials are very closely matched in the aspect of strength standards used for design. The difference between these materials that is apparent in Figure 30 are the amounts of elongation until fracture. This will be discussed in Section 6.2.

The next important point of discussion to be brought up from testing is the variance in the strength data collected from each material. As can be seen in Figures 8 & 9 the variance of yield loads for titanium 6-4 are greater than A286. This is also shown in the box plots in Figure 11. As can be seen in Figure 11 as well, there are two outliers for titanium 6-4 which are well out of range while only one outlier misses the A286 grouping by narrower margin. These two extremes that read low on the titanium 6-4 data were the first two tests conducted so they might be off due to the machine warming up to operating temperature. The A286 that is labeled an extreme however was 14<sup>th</sup> in the test order so it cannot be attributed to the load frame warming up. Even if these extremes are ignored the 25<sup>th</sup> to 75<sup>th</sup> quartile variance is greater for the titanium than the A286. Even with this variance and extremes the A286 specimens all passed the 5,100 lb. tensile load carrying capabilities stated in NASM 1312-8 as the certification sheets documented.

## **6.2 Ductility Index**

As stated in the previous Section 6.1, the strengths of these two materials were closely matched but the noticeable difference is in the amount of elongation each material went through between when it yielded to when it fractured. As can be seen in Table 4 of Chapter 4 the ductility index for A286 was on average ten times greater than the titanium 6-4 specimens. Even looking

at the maximum of the titanium 6-4 compared to the minimum of the A286 the ductility indexes are still almost ten times different.

If Figure 19 is viewed once more, the bottom box of the flow chart deals with a ductility index calculation. If the ductility index is greater than 0.25 then separation may occur before rupture if all other criteria are met. However, if ductility index is less than 0.25 rupture may occur first. This last condition of the flow chart dealing with ductility index is determining the brittleness of a fastener. This ductility index of 0.25 is taken to be the parting line between brittle and ductile fasteners. Even though the A286's ductility index is on average ten times greater than that of titanium 6-4 the titanium alloy still is greater than this 0.25 value from the flow chart and will move the user of the flow chart to the separation before rupture section to determine margin of safety calculations. This means by the NASA 5020 [7] flow chart standard, the titanium 6-4 is ductile enough to not be considered a brittle fastener.

The final point to reiterate is the manner in which each fastener broke in testing. From Figure 13 you can see the flat fracture which was perpendicular to the axis of loading, breaking only across one thread. This is indicative of a brittle material when a tensile load is applied. On the other hand, Figure 14 shows the fracture of A286. As can be seen the fracture is across multiple threads and much closer to a 45° plane than the titanium 6-4. Again, this is a characteristic of a more ductile fracture when the loading is in tension.

### **6.3 Joint Diagram Examples**

A total of 18 joint diagram examples were worked through to see how these two materials would perform in different preload and external load scenarios. The preload values, as stated in Section 5.2, are based off of minimum yield strength values collected during testing for this thesis. From these preload values an external load was placed on the system which is half of

the nominal preload value since this is considered good joint design. The flow chart in Figure 19 was used for all joint diagram examples to determine if joint separation or rupture would occur first. If separation occurs first, as it does for all joint diagram examples except one, the load on the bolt was found for when the joint would separate since at this point the bolt would see the full external load. This load at joint separation was then multiplied by 1.4 to obtain a 40% safety margin. This safe load was then compared to the minimum tensile strength of the data collected for this thesis to determine if that joint diagram example was safe to use. Table 7 below is much like Table 6 and will go over the outcomes for each joint diagram example.

Table 7 - Joint Diagram Example Results

Loading Plane	Joint Diagram Example	Titanium 6-4	A286
Half Loading Planes	115% Example (90% + 25% Torque Uncertainty)	Only case where rupture will occur before separation	Separation before rupture does not meet 40% safety margin
	Nominal 90%  Example	Does not meet 40% safety margin but does meet a 20% margin	Does not meet 40% safety margin but does meet a 20% margin
	65% Example (90% - 25% Torque Uncertainty)	Pass with 40% Safety Margin	Pass with 40% Safety Margin
	90% Example (65% + 25% Torque Uncertainty)	Does not meet 40% safety margin but does meet a 20% margin	Does not meet 40% safety margin but does meet a 20% margin
	Nominal 65%  Example	Pass with 40% Safety Margin	Pass with 40% Safety Margin
	40% Example (65% - 25% Torque Uncertainty)	Pass with 40% Safety Margin	Pass with 40% Safety Margin

Table 7 (Continued)

Full Loading Planes	90% Example (65% + 25% Torque Uncertainty)	Does not meet 40% safety margin but does meet a 20% margin	Does not meet 40% safety margin but does meet a 20% margin
	65% Example	Pass with 40% Safety Margin	Pass with 40% Safety Margin
	40% Example (65% - 25% Torque Uncertainty)	Pass with 40% Safety Margin	Pass with 40% Safety Margin

The takeaways from Table 7 above are how these fasteners will perform at each preload level. At the upper end of uncertainty for the nominal 90% joint diagram example both the A286 and titanium 6-4 will not meet safety margin when the joint separates and the titanium alloy in this case will actually fail before the joint separates. The 90% preload level, no matter what the external load, will not obtain 40% safety margin, however, a 20% margin can be met at the point of joint separation. At a preload level of 65% and 40%, and either external load, the joint diagram examples show that the bolt will meet a 40% margin of safety for these cases. It is important to note in all of these examples that they are very controlled scenarios and so they should be treated as such. In operations external loads are rarely exactly what they were designed for. These examples are to provide a general idea of how each fastener will perform under ideal loading and preloading scenarios

.

## CHAPTER 7: CONCLUSIONS

After tensile testing was conducted, yield and tensile strengths were determined and the ductility indexes calculated. It was found that the yield and tensile strength of the titanium 6-4 was similar to that of A286. The difference between yield and tensile strength of the titanium alloy was smaller though with around 20,000 psi more stress being carried after yield strength before its tensile strength was reached. The A286 on the other hand was able to withstand twice that on average with 43,000 psi between the yield and tensile stress values. The ductility index of the A286 however was, on average, ten times greater than the titanium 6-4.

Joint diagrams were then constructed and analyzed for reasonable preload and external loading conditions. This large difference in ductility index did not hinder the performance of the titanium alloy in all but the highest preloading joint diagram example. A flow chart was worked through for all joint diagram examples to see if the joint will separate first or if the fastener will rupture before separation. If the preload on the fasteners is 115% of minimum yield strength, seen in testing for this thesis, the titanium alloy will rupture before the joint separates. The A286 in this same example will separate before rupture but 40% safety margin will not be achieved. Both bolts perform similarly in all other loading examples gone through. At 90% preload the joints will separate before rupture but only a 20% safety margin is obtained at separation. At 65% and 40% preload of minimum yield strength however both materials will obtain a 40% safety margin at the point of joint separation.

Overall, the testing shows that titanium 6-4 fasteners can be used safely if proper joint design is taken into account and torque-preload equivalence uncertainty is minimalized. This uncertainty can be reduced by using proper lubricants when installing the bolts and using instrumented fasteners.

Constructing joint diagram examples with the preload and external loads the joint is designed to handle in service is also good practice to see if joint separation or bolt rupture will occur first and determine if acceptable safety margins can be met. This thesis and the data collected helps fill a void in the literature on titanium 6-4 fasteners compared to more conventional A286 for aerospace and aeronautical fields.

## REFERENCES

- [1] “Titanium Grade Overview”, Supra Alloys Inc. 2013. Web. 11 November 2013  
<<http://www.supraalloys.com/titanium-grades.php>>
- [2] Williams J, Starke Jr. EA. Progress in structural materials for aerospace systems. *Acta Materialia* Inc. 2003;51:5775-5799
- [3] Costa M.Y.P, Venditti M.L.R, Cioffi M.O.H, Voorwald H.J.C, Guimaraes V.A, Ruas R. Fatigue behavior of PVD coated Ti-6Al-4V alloy. *International Journal of Fatigue* 2011;33: 759-765
- [4] “A-286 Technical Data”, High Temp Metals. Web. 11 November 2013  
<<http://www.hightempmetals.com/techdata/hitempA286data.php>>
- [5] Gurrappa I. Characterization of titanium alloy Ti-6Al-4V for chemical, marine and industrial applications. *Materials Characterization* 2003;51:131-139
- [6] Gorynin I.V. Titanium alloys for marine application. *Materials Science and Engineering* 1999;A263:112-116
- [7] National Aeronautics and Space Administration (NASA) STD-5020: Requirements for Threaded Fastening Systems in Spaceflight Hardware. 2012.
- [8] Stevenson M.E, McDougall J.L, Cline K.G. Metallurgical Failure Analysis of Titanium Wing Attachment Bolts. *Practical Failure Analysis*. August 2003, Vol. 3(4).
- [9] De Matteis G, Landolfo, R. *Mechanical Fasteners for Cladding Sandwich Panels: Interperative models for Shear Behavior*, *Thin-Walled Structures* 1999;35:61-79
- [10] Jung G.S, Lee K.Y, Lee J.B, Bhadeshia H.K.D.H, Suh D.-W. *Spot Weldability of TRIP Assisted Steels with High Carbon and Aluminum Contents*. *Science and Technology of Welding and Joining* 2012; Vol.17 No.2; 92-99
- [11] Samuel K.G, *Dependence of Strength and Ductility Ratios in Austenitic Stainless Steels*. *International Journal of Pressure Vessels and Piping* 2006;83:474-476
- [12] Maghsoudi A.A, Bengar H.A. *Moment Redistribution and Ductility of RHSC Continuous Beams Strengthened with CFRP*. *Turkish J. Engineering Enviromental Science* 2009;33:45-49
- [13] Ashour A.F, El-Refaie S.A, Garrity S.W. *Flexural Strengthening of RC Continuous Beams Using CFRP Laminates*. *Cement & Concrete Composites* 2004;26:765-775



- [14] Munoz W. Salenikovich A. Mohammad M. Quenneville P. *Determination of Yield Point and Ductility of Timber Assemblies: In Search for a Harmonised Approach*. Quebec, Canada.
- [15] Lin Shin-Hua, Pan Chi-Ling, Hsu Wei-Ting. *Monotonic and Cyclic Loading Tests for Cold-Formed Steel Wall Frames Sheathed with Calcium Silicate Board*. *Thin-Walled Structures* 2014;74:49-58
- [16] Dolan J.D, "Proposed Test method for Dynamic, Properties of Connections Assembled with Mechanical Fasteners," *Journal of Testing and Evaluations, JTEVA*, Vol.22 No. 6, November 1994, pp. 542-547.
- [17] Venkateswarlu V, Tripathy D, Rajagopal K, Tharian K.T, Venkitakrishnan P.V. Failure analysis and optimization of thermo-mechanical process parameter of titanium alloy (Ti-6Al-4V) fasteners for aerospace applications. *Case Studies in Engineering Failure Analysis* 2013;1:49-60
- [18] Hopple, George. Shear band failures in threaded titanium alloy fasteners. *American Society of Metals* 1985;12:474-485
- [19] Stevenson M.E, McDougall J.L, Cline K.G, *Metallurgical Failure Analysis of Titanium Wing Attachment Bolts*. PFANF8 2003;4:75-80
- [20] Jha, Abhay K, Singh Satish Kumar, Kiranmayee M. Swathi, Sreekumar K, Sihna P.P. Failure analysis of titanium alloy (Ti6Al4V) fastener used in aerospace application. *Engineering Failure Analysis* 2010;17:1457-1465
- [21] Gross, Fred. "Concerns with the Use of Titanium Fasteners". *NASA Materials Engineering Branch: TIP\* No.133*. June 2003.
- [22] Meyer Gerhard, "Simple Diagrams aid in Analyzing Forces in Bolted Joints". *Assembly Engineering: Fastening and Joining*, January 1972: 28-33
- [23] Meyer Gerhard, "How to Calculate Preload Loss Due to Permanent Set in Bolted Joints". *Assembly Engineering: Fastening and Joining* February 1972: 30-34
- [24] Nicholas T. *Dynamic Tensile Testing of Structural Materials Using a Split Hopkins Bar Apparatus*, Air Force Wright Aeronautical Laboratories. October 1980.
- [25] Barret, Craig R., Nix, William D., Tetelman, Alan S. *The Principles of Engineering Materials*. Englewood Cliffs, New Jersey: Prentice-Hall Inc., 1973. Print.
- [26] American Society for Testing and Materials (ASTM) F606-13: *Standard Test Methods for Determining the Mechanical Properties of Externally and Internally Threaded Fasteners, Washers, and Rivets*. 2013.
- [27] Montgomery, Douglas C, *Design and Analysis of Experiments 6<sup>th</sup> Ed*. Chapter 2, Section 4.2. John Wiley & Sons, Inc. 2005. Print.
- [28] Chambers, Jeffrey A., *NASA Technical Memorandum 106943. Preloaded Joint Analysis Methodology for Space Flight Systems*. 1995.

- [29] Verein Deutscher Ingenieure (VDI) 2230: Systematic Calculation of High Duty Bolted Joints, Joints with Once Cylindrical Bolt. 2003.
- [30] Wanhill, R., Barter, S. Fatigue of Beta Processed and Beta Heat-treated Titanium Alloys. Springer. 2012. Print.
- [31] U.S. Department of Transportation – Federal Highway Administration, *Publication Number: FHWA-RD-02-095 Appendix G*. April 2012. Web.
- [32] Aerospace Specification Metals, Inc. *Titanium Ti 6AL 4V – AMS 4911*. June 2015. Web.
- [33] Carpenter Technology Corporation. *Pyromet Alloy A286 – Tensile Properties*. June 2015. Web.
- [34] American Society of Testing and Materials (ASTM) E8M-01 Standard Test Methods for Tension Testing of Metallic Materials [Metric]. 2004.

## **APPENDIX A: HEAT TREATMENTS**

### **A.1 A286 Heat Treatment**

The A286 is produced by Ugitech Groupe for Techalloy Union per specification D.3.PRS.010.S/REV.E. At the time of shipment it was 0.295 inch diameter A286 rod and passed its chemical composition and the heat treatment specifications and condition of delivery was stated. Three V Fasteners purchased this stock now 0.2465 inches in diameter from Techalloy. It was then sent to Continental Heat Treating, Inc. where it was solution treated at 1800 degrees Fahrenheit for 2 hours then oil quenched and then age hardened at 1325 degrees Fahrenheit for 16 hours. This took the bolts to a 130 Ksi minimum tensile strength. 3V Fasteners then performed final inspection along with performing stress rupture and tensile tests before shipping to Wesco Aircraft. These fasteners were then purchased through Aerolyusa Inc. for our testing. All these transactions and test results were provided from Aerolyusa when the shipment arrived.

### **A.2 Titanium 6-4 Heat Treatment**

The Titanium 6-4 fasteners were obtained gratis from SPS Technologies in Jenkintown, PA. They had purchased and produced the bolts to test locking nuts that they added to their product line but only used 3 bolts of the 50 specimen lot and the remaining were left in inventory. The bar stock was purchased by SPS from Dynamet, Inc. and the certification

was provided. The following table shows the processing steps that SPS took to produce the bolts from the bar stock which took the alloy to a 160 ksi minimum tensile strength.

Table A- Titanium 6Al-4V Bolt Manufacturing Procedure

1	Cut Bars to Proper Length
2	Forge Heads
3	Solution Treat (1710°F / 30 minutes)
4	Vacu Blast
5	Straighten
6	Age Harden (950°F for 4 hours)
7	Vacu Blast
8	Machine Head
9	Machine to Length
10	Stamp Head with Shop Order and Lot Number
11	Grind Body and Under-Head
12	Grind Thread Roll Diameter
13	Roll Threads
14	Grind Thread Major Diameter
15	Apply Cetyl alcohol Grade B

This heat treatment process leaves the grain structure as depicted in the figure below. The beta grains that were formed decomposed into the transformed alpha structure that can be seen in the lamellae layers of the beta grains. Looking back at the phase diagram from the Background section as the temperature increases the primary alpha decreases as the alloy nears its beta transus temperature. However, as the temperature increases the percentage of Vanadium, the beta stabilizer, decreases. Upon cooling since there is less Vanadium the beta phase that had formed at the higher temperature more easily transforms to alpha phase making the lamella layers seen below since the beta phase is unstable at lower temperatures.

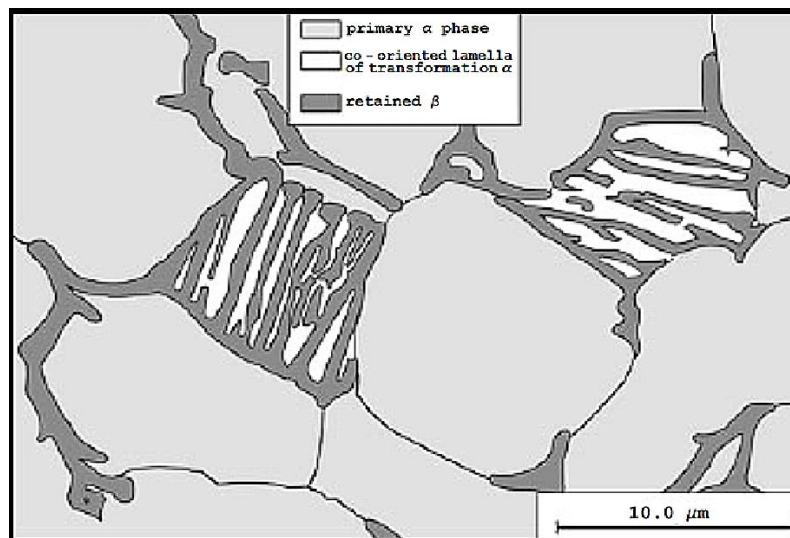


Figure A: Titanium 6Al-4V Grain Structure with Heat Treatment. Reprinted from “Metallurgy and Microstructure” by Wanhill,R., and Barter, S., 2012, Fatigue of Beta Processed and Beta Heat-Treated Titanium Alloys, pg. 7 Copyright 2012 by Springer Reprinted with permission.

## APPENDIX B: CHOICE OF SAMPLE SIZE

Montgomery [34] was used to determine the proper sample size for testing. The tensile testing done is a single factor experiment, which is the material difference. As stated, the choice of sample size is very important and the concern is “wrongly failing to reject the null hypothesis” ( $H_0: \mu_1 = \mu_2$ ) that the variables being tested are equal to each other. An operating characteristic curve with a significance level of 0.05 as shown below in Figure A is also used. It assumes that the population variance is unknown but equal along with the assumption that the sample sizes are equal.

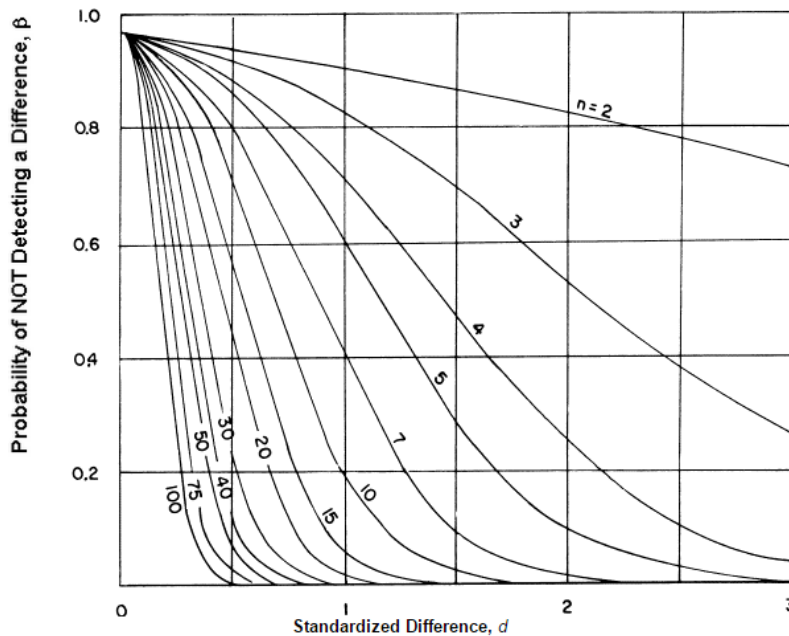


Figure B: Operating Characteristic Curve [31]

The two parameters on the axis are  $d$  and Beta, or the probability of failing to reject the null hypothesis. The axis labeled ‘ $d$ ’ is the standardized difference in the variable of interest in the experiment, which is the ductility index. Since no relevant data of ductility index for these two materials were found the elongation to fracture of the materials were used as a basis. Titanium 6-4 to AMS 4928 specification, like that of the fasteners used, have 14% elongation to fracture [32] and A286 to AMS 5731, like that of the fasteners used, has 24% elongation to failure [33]. These values were used as  $\mu_1$  and  $\mu_2$  in the equation below. The standard deviation  $\sigma$  is not known before testing begins so this value needs to have an educated guess to input and 5% deviation was thought to be reasonable.

$$d = \frac{|\mu_1 - \mu_2|}{2\sigma} \quad (1)$$

Calculating  $d$  from Equation 1 yields a value of 1. An acceptable error of 5%,  $\beta=0.05$ , is decided to be acceptable and then Figure B is looked at to find the value of  $n^*$  which are the lines on the graph. This comes out to be approximately 16. This value of  $n^*$  however is not the sample size since it is equal to two times the sample size minus one. Therefore, solving this gives a sample size of 8.5 which is rounded up to 9. A slightly larger sample size of 12 however was chosen to make up for the uncertainty in guessing the standard deviation of the elongation in Equation 1.

After testing was completed this calculation was carried out again with the ductility indexes from Table 4 along with computed standard deviation. The difference on average is 5 between the A286 and titanium 6-4 ductility indexes and the A286 has the greater standard deviation at around 0.3. The result for the standardized difference came out to be 8.3 which is well off the chart. This makes it apparent that the twelve samples is over a necessary testing

population to have statistically meaningful results. This makes sense because the averages of the two materials are so far apart and this test is to make sure they are not thought to be the same, which is the null hypothesis.



## APPENDIX C: DUCTILITY INDEXES

As stated previously the ductility index will be defined from NASA STD-5020 Appendix A.5 [7]. It is stated to be the displacement in the plastic range over the displacement in the elastic range. Below will be each of the 24 tests run which the ductility index was taken from. The elastic range is best estimated from the graph and the end of the plastic range is taken from the test data.

### C.1 Titanium 6-4 Ductility Index

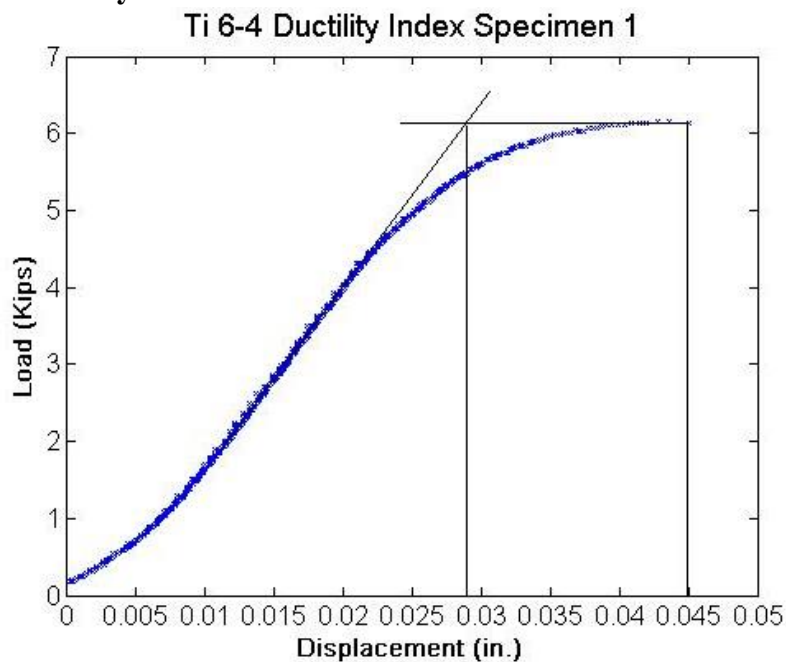


Figure C: Titanium 6-4 Ductility Index Specimen 1

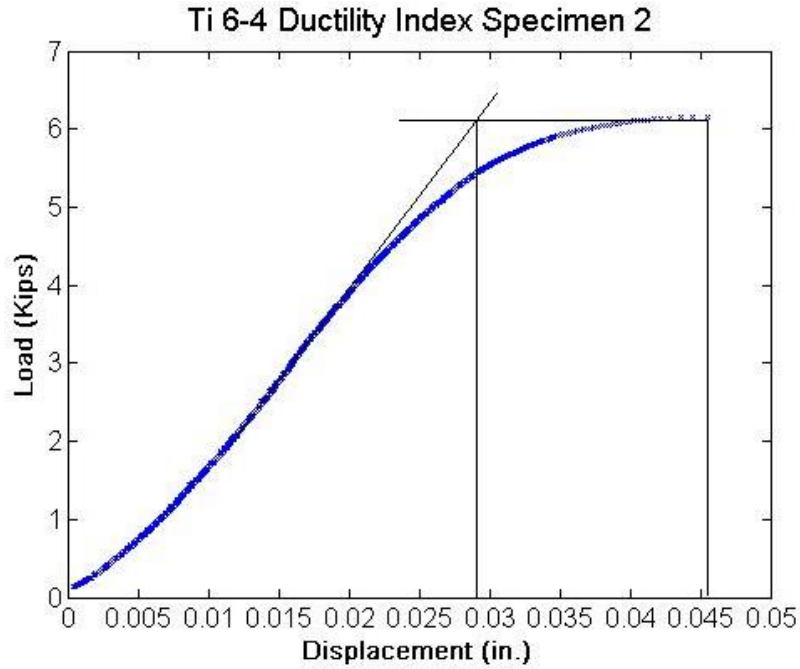


Figure D: Titanium 6-4 Ductility Index Specimen 2

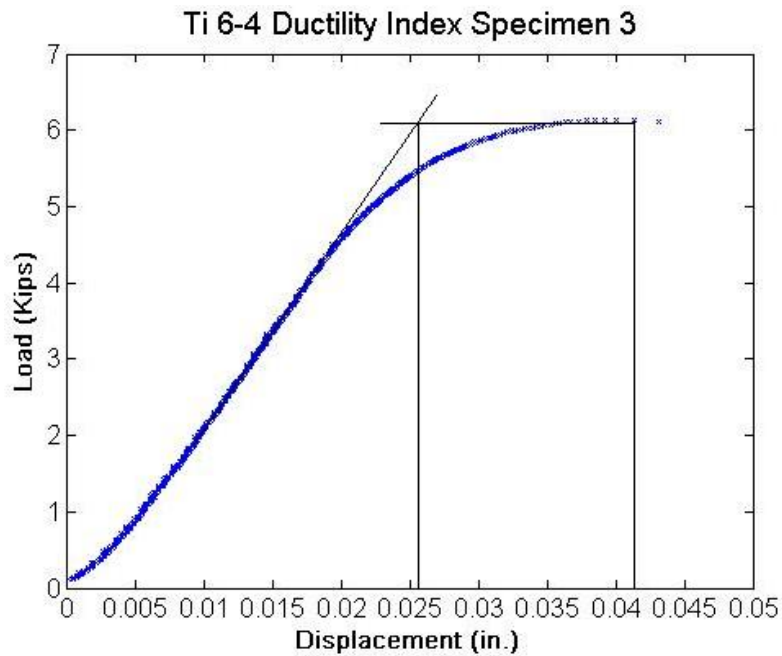


Figure E: Titanium 6-4 Ductility Index Specimen 3

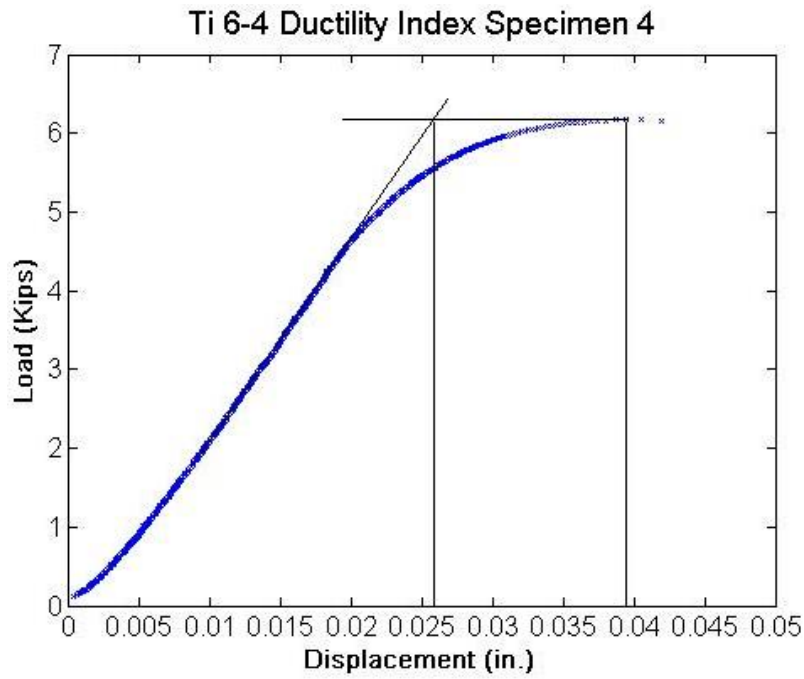


Figure F: Titanium 6-4 Ductility Index Specimen 4

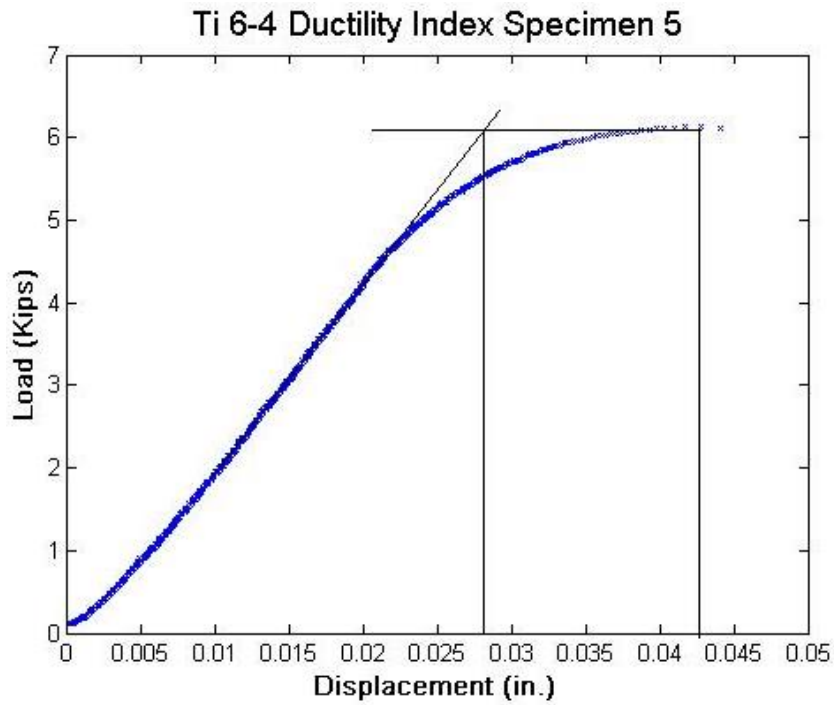


Figure G: Titanium 6-4 Ductility Index Specimen 5

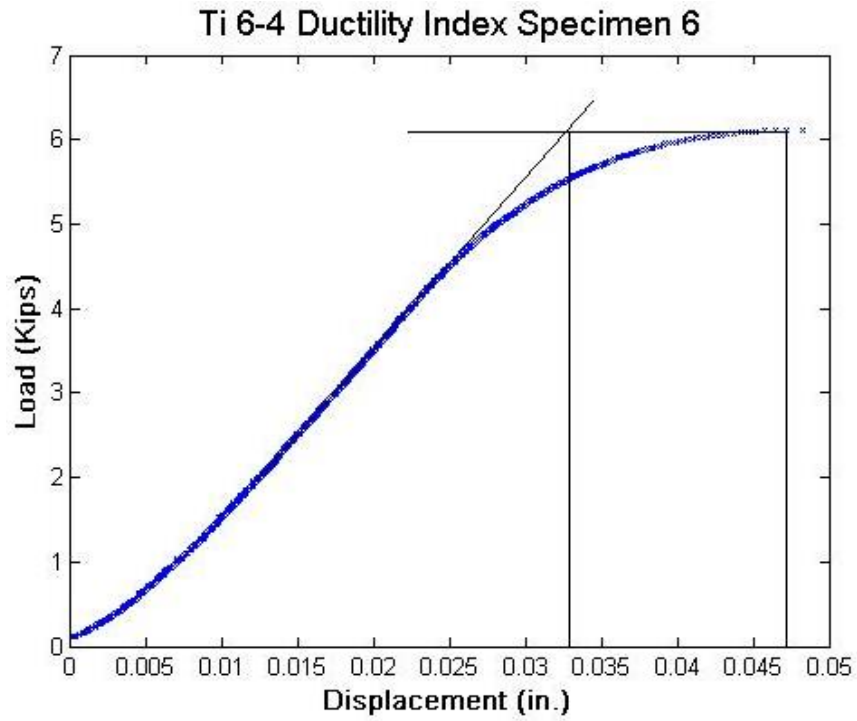


Figure H: Titanium 6-4 Ductility Index Specimen 6

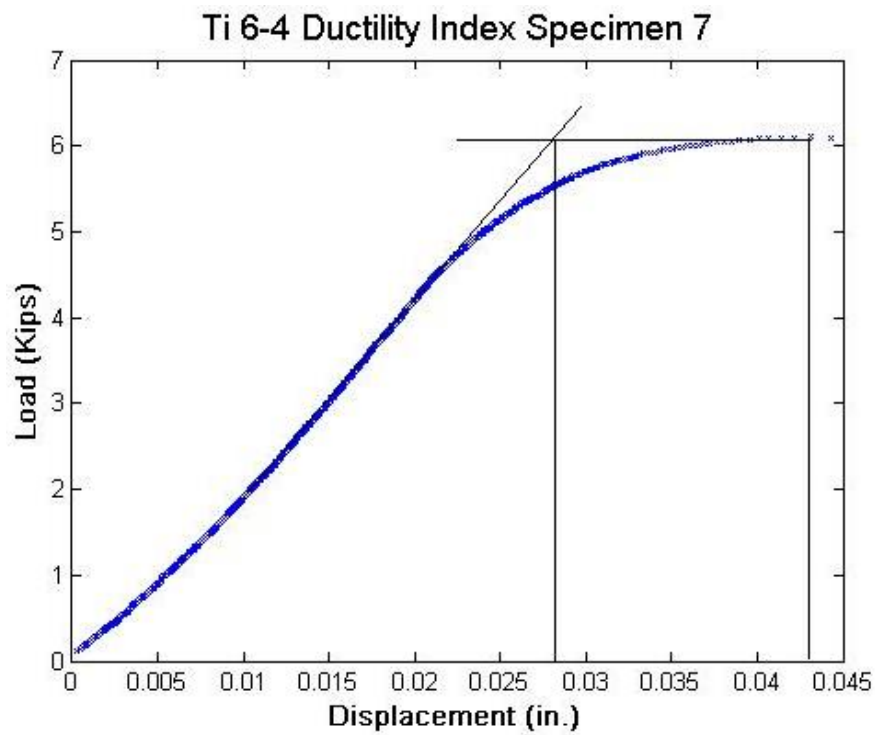


Figure I: Titanium 6-4 Ductility Index Specimen 7

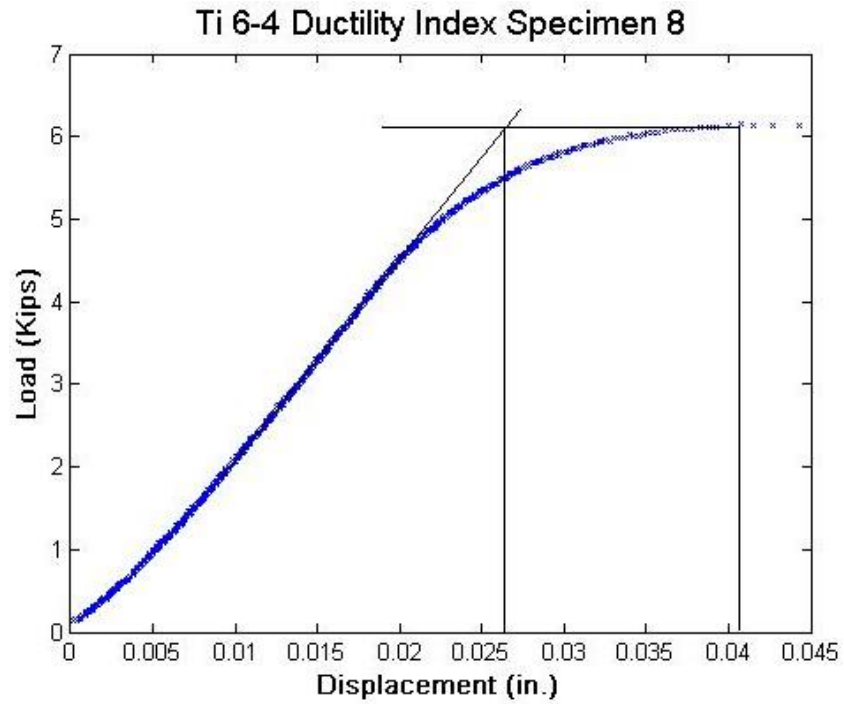


Figure J: Titanium 6-4 Ductility Index Specimen 8

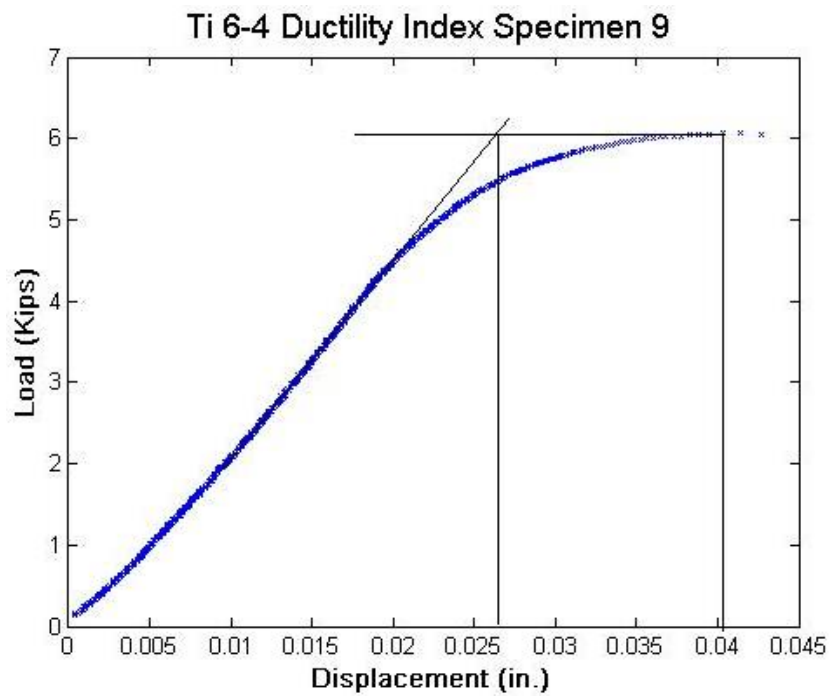


Figure K: Titanium 6-4 Ductility Index Specimen 9

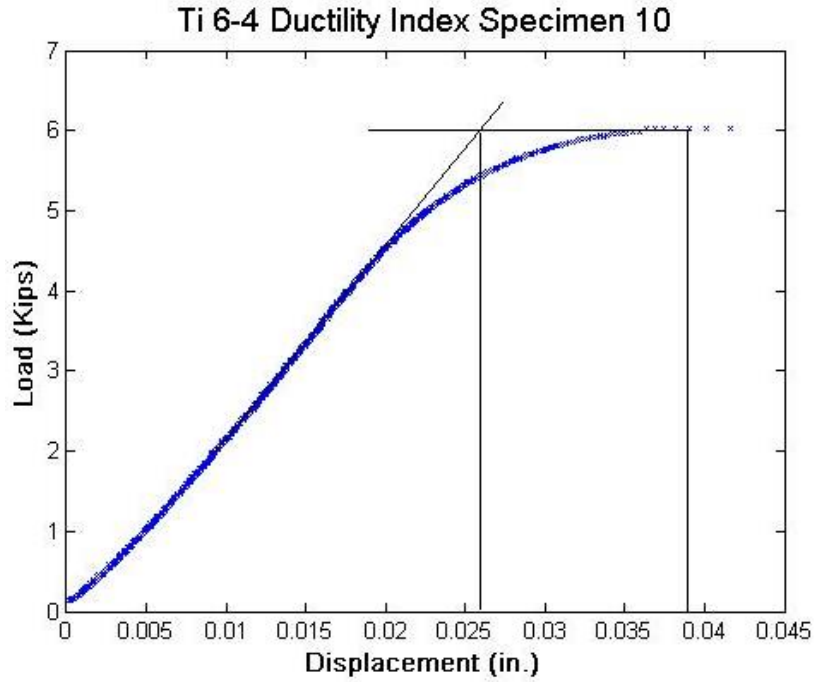


Figure L: Titanium 6-4 Ductility Index Specimen 10

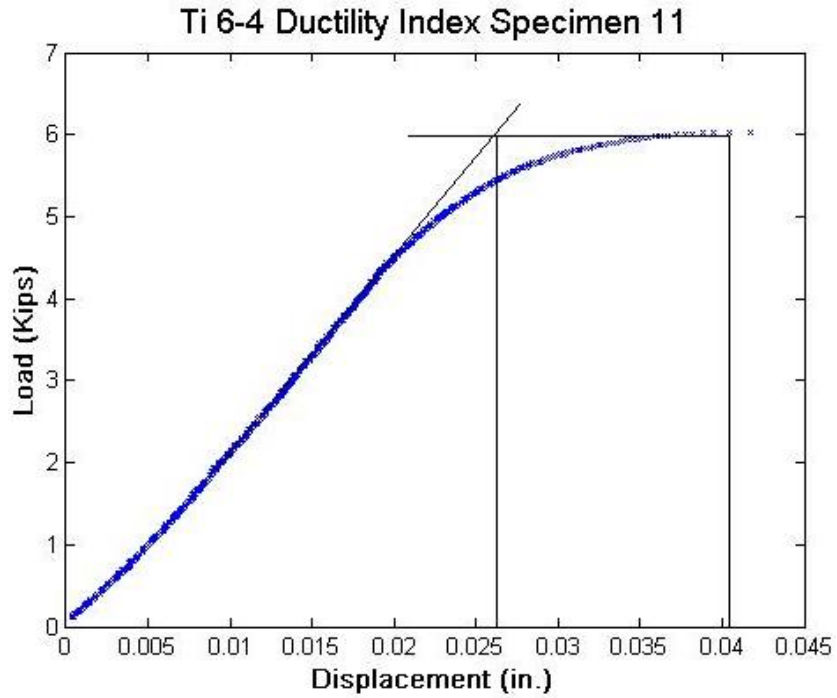


Figure M: Titanium 6-4 Ductility Index Specimen 11

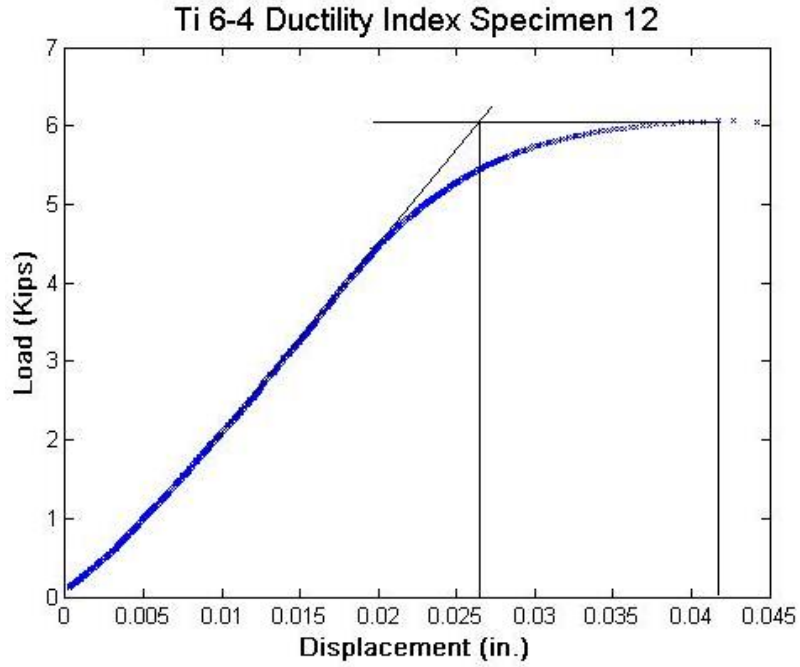


Figure N: Titanium 6-4 Ductility Index Specimen 12

### C.2 A286 Ductility Index

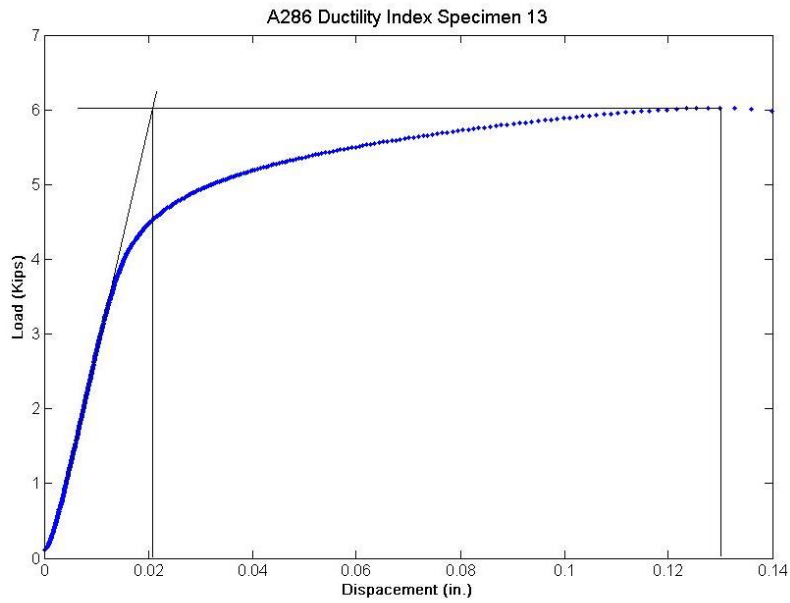


Figure O: A286 Ductility Index Specimen 13

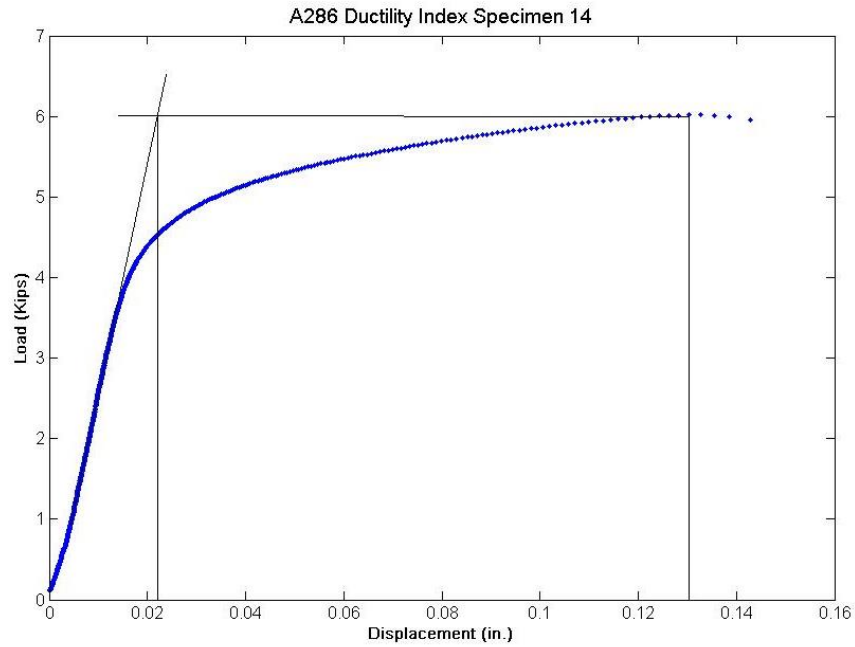


Figure P: A286 Ductility Index Specimen 14

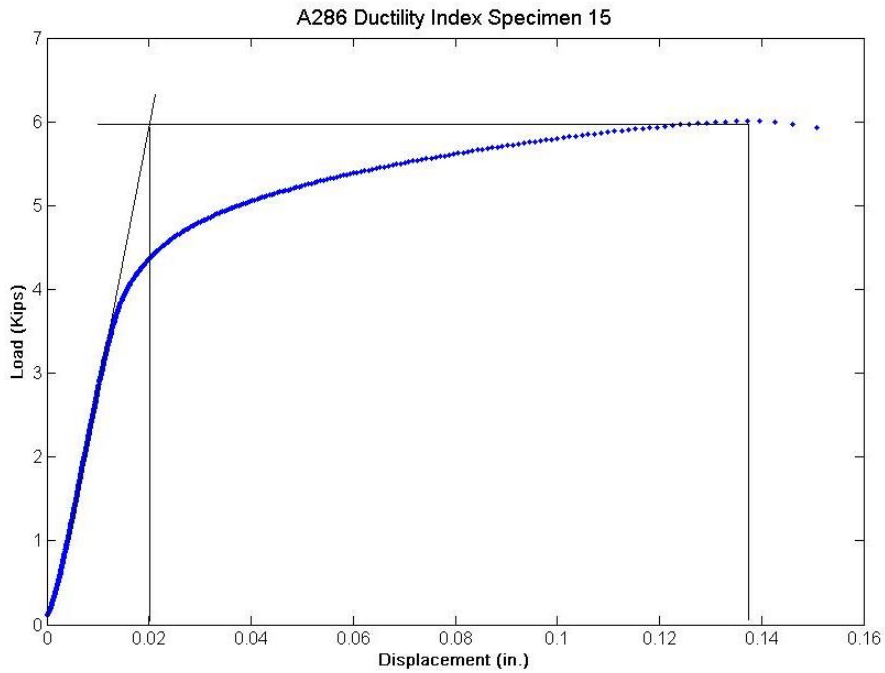


Figure Q: A286 Ductility Index Specimen 15



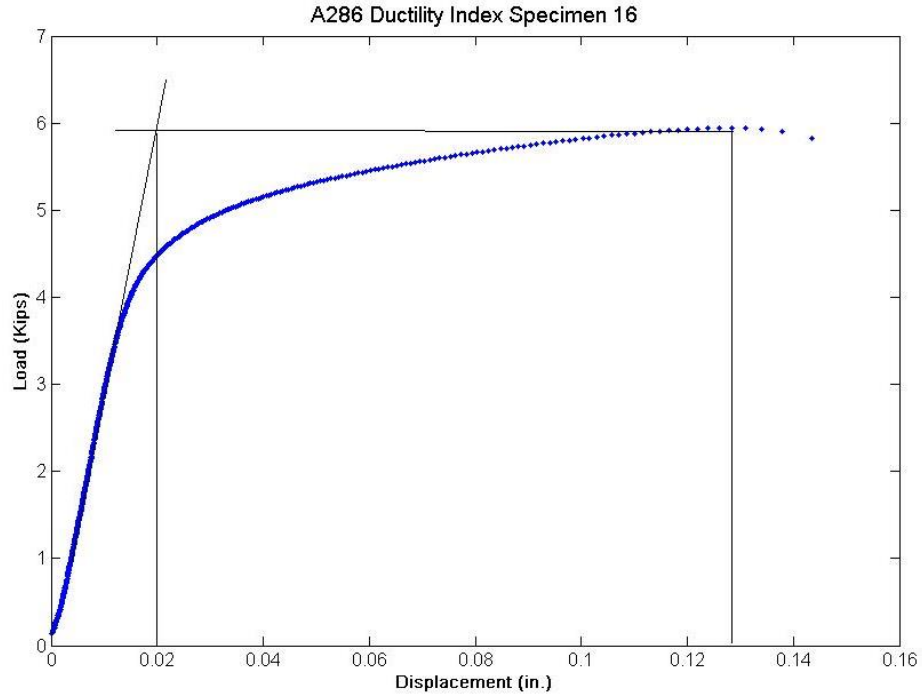


Figure R: A286 Ductility Index Specimen 16

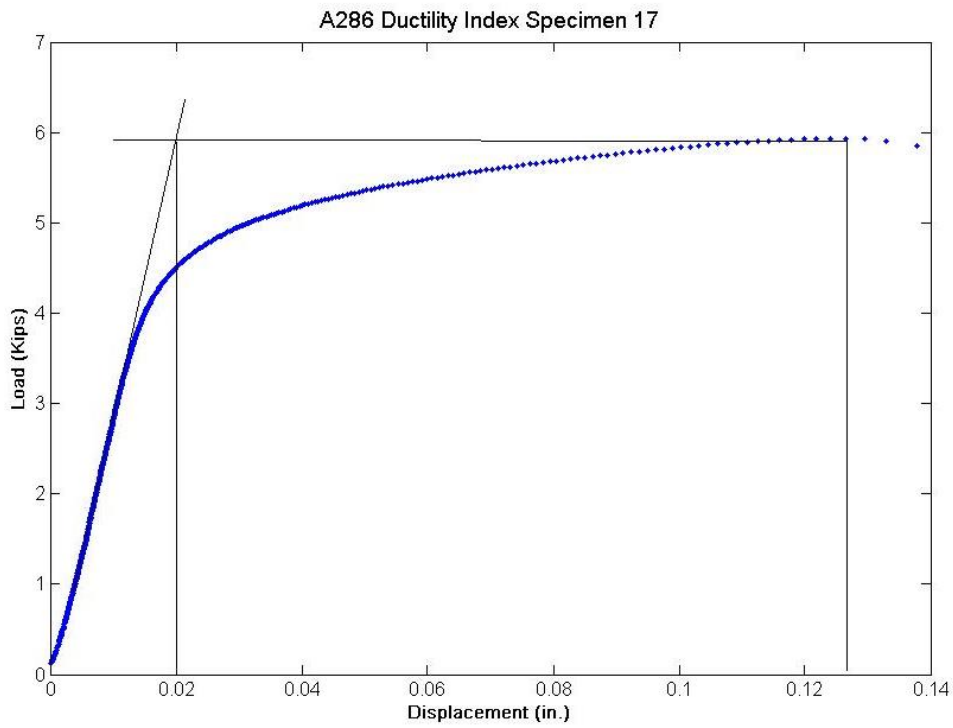


Figure S: A286 Ductility Index Specimen 17

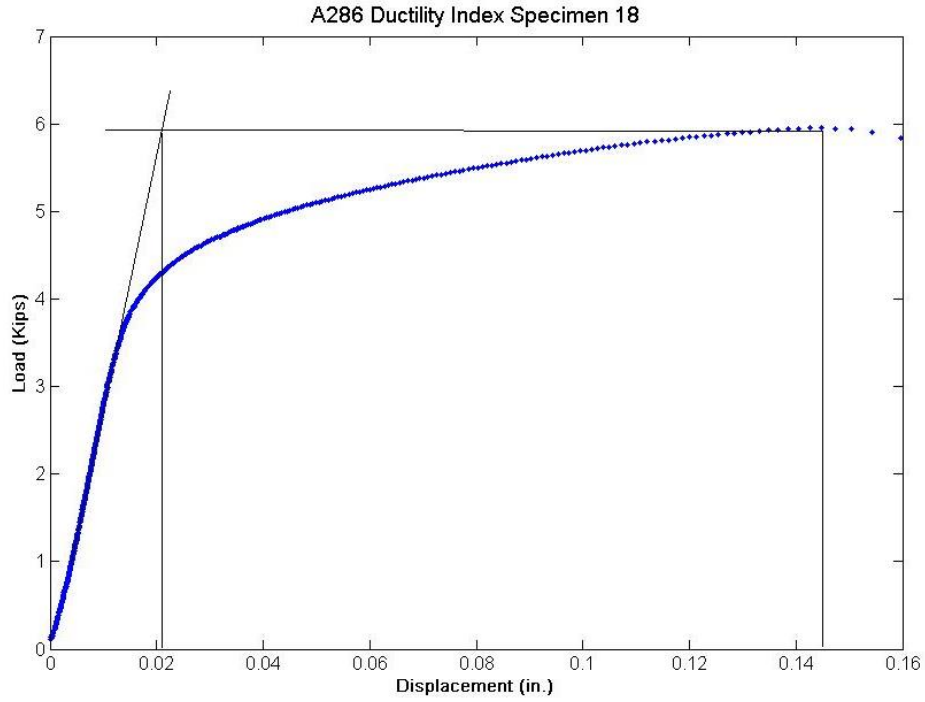


Figure T: A286 Ductility Index Specimen 18

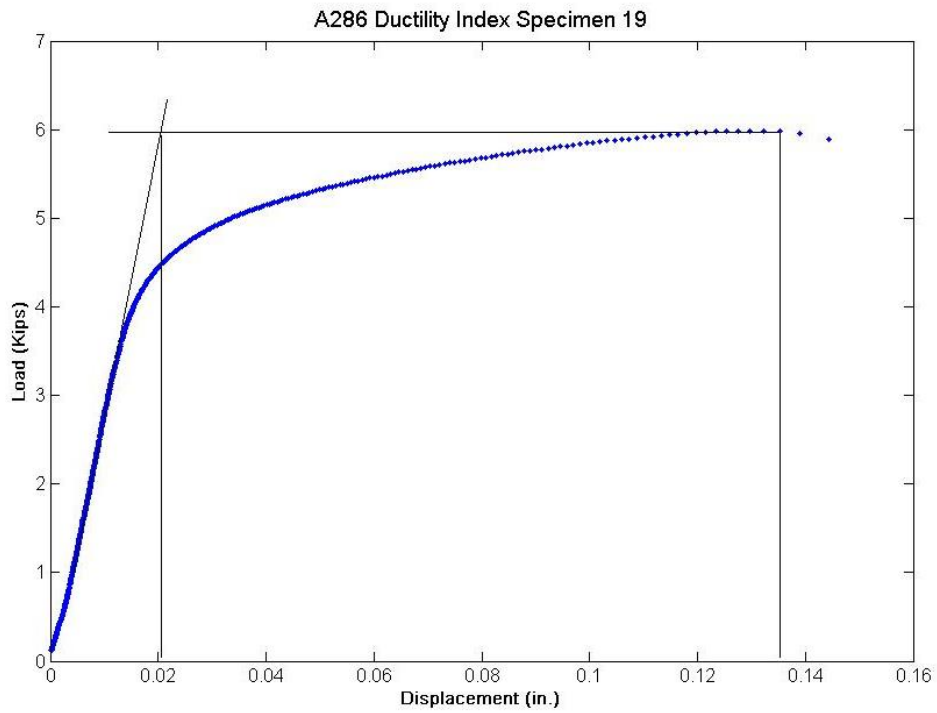


Figure U: A286 Ductility Index Specimen 19

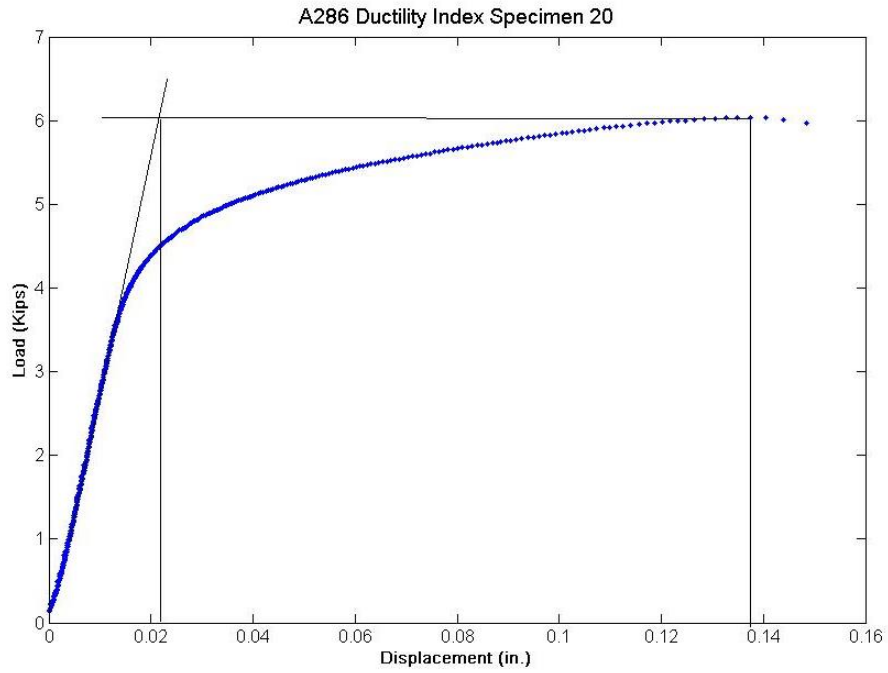


Figure V: A286 Ductility Index Specimen 20

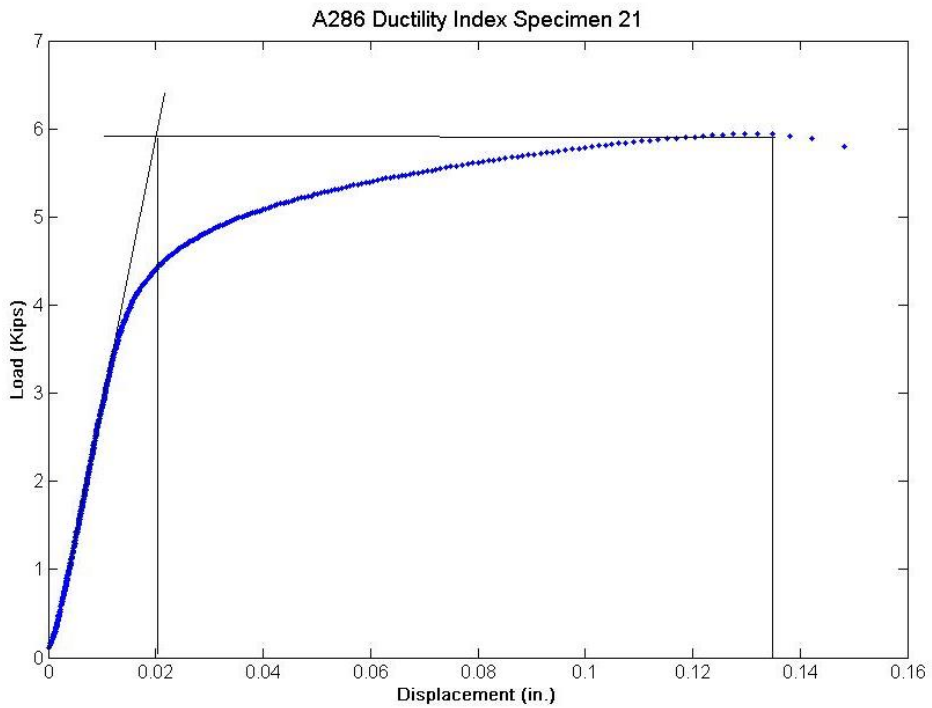


Figure W: A286 Ductility Index Specimen 21

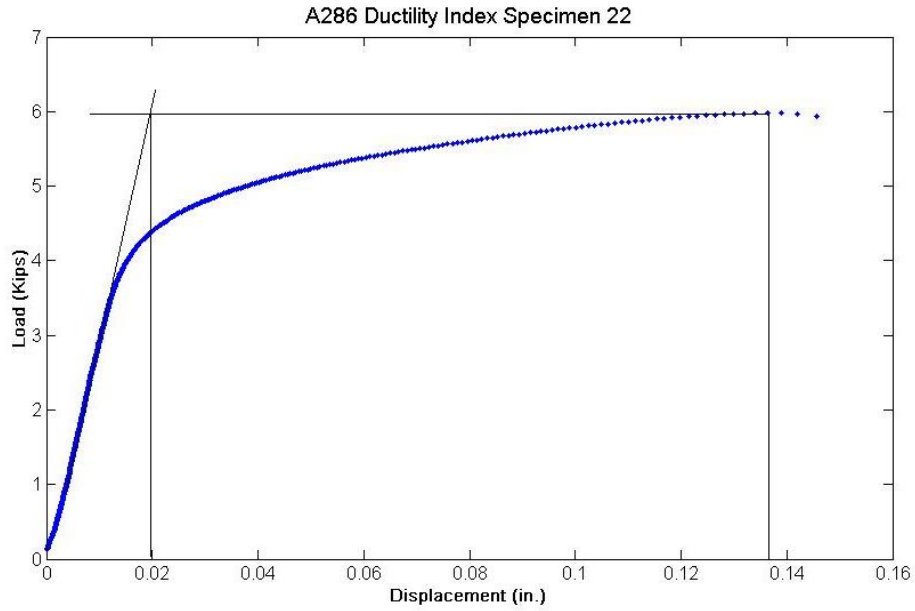


Figure X: A286 Ductility Index Specimen 22

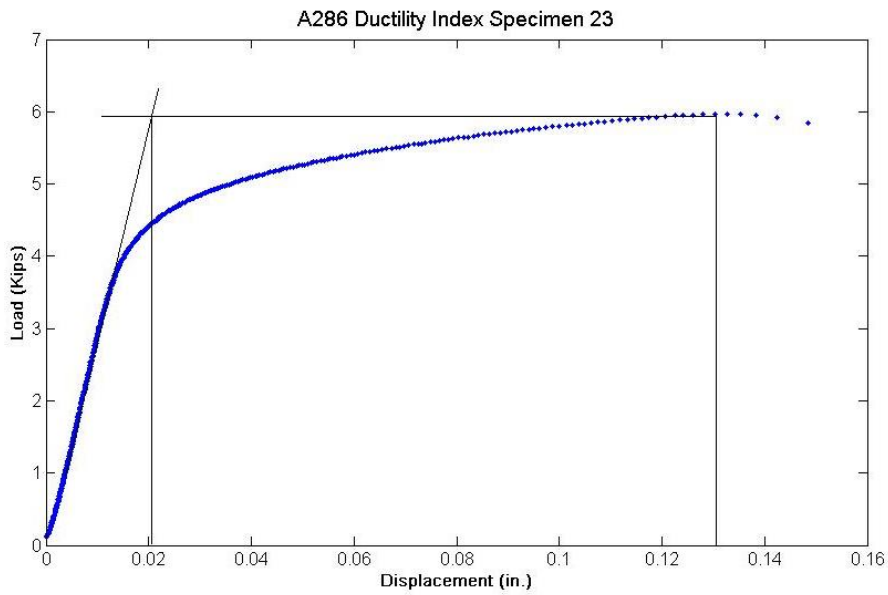


Figure Y: A286 Ductility Index Specimen 23

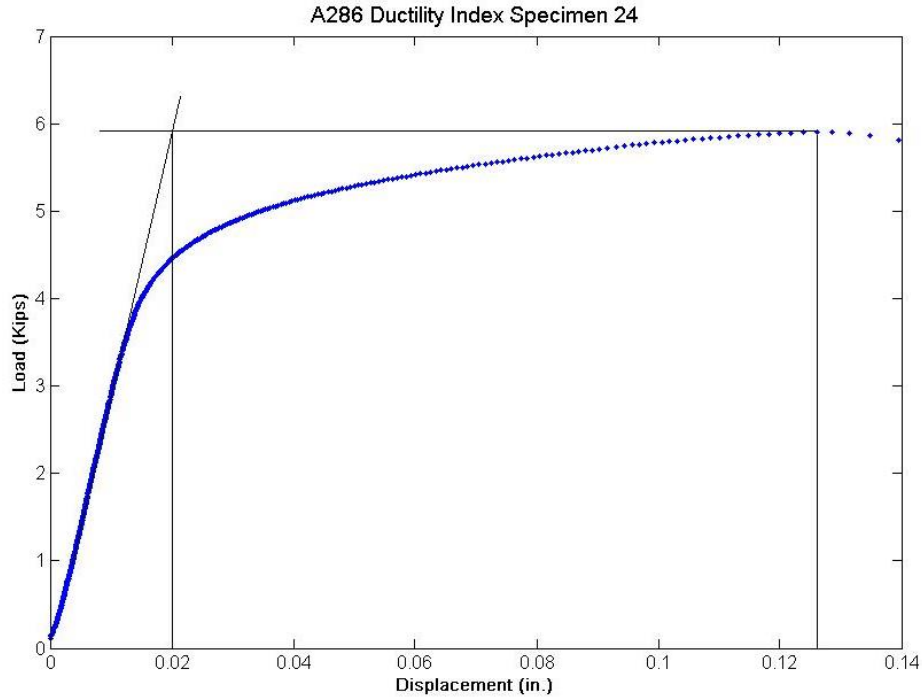


Figure Z: A286 Ductility Index Specimen 24

Table B- Ductility Index Calculations

Specimen Number	Elastic Range	Plastic Range	Ductility Index
Ti 6-4 Specimen 1	0.028	0.0435	0.554
Ti 6-4 Specimen 2	0.028	0.0444	0.586
Ti 6-4 Specimen 3	0.026	0.0385	0.481
Ti 6-4 Specimen 4	0.026	0.0395	0.519
Ti 6-4 Specimen 5	0.027	0.0428	0.585
Ti 6-4 Specimen 6	0.033	0.0472	0.43
Ti 6-4 Specimen 7	0.028	0.0431	0.539
Ti 6-4 Specimen 8	0.026	0.0407	0.565

Table B (Continued)

Ti 6-4 Specimen 9	0.026	0.0404	0.554
Ti 6-4 Specimen 10	0.026	0.0381	0.465
Ti 6-4 Specimen 11	0.026	0.0405	0.558
Ti 6-4 Specimen 12	0.027	0.0417	0.544
A286 Specimen 13	0.021	0.130	5.19
A286 Specimen 14	0.022	0.133	5.05
A286 Specimen 15	0.02	0.137	5.85
A286 Specimen 16	0.02	0.126	5.3
A286 Specimen 17	0.02	0.127	5.35
A286 Specimen 18	0.021	0.145	5.9
A286 Specimen 19	0.021	0.127	5.05
A286 Specimen 20	0.022	0.138	5.27
A286 Specimen 21	0.02	0.132	5.6
A286 Specimen 22	0.02	0.136	5.8
A286 Specimen 23	0.021	0.130	5.19
A286 Specimen 24	0.02	0.126	5.3

## APPENDIX D: SPRING CONSTANT CALCULATIONS

### D.1 Bolt Spring Constant

To calculate the spring constant of the bolt the following equation was pulled from the Meyer's paper [22]:

$$\frac{1}{K_B} = \frac{1}{E} \left( \frac{0.4d}{A_s} + \frac{l_s}{A_s} + \frac{l_t}{A_t} + \frac{0.4d}{A_t} \right) \quad (2)$$

In this equation E is the Young's Modulus of the bolt,  $A_s$  is the stress area of the shank which is calculated from equation 1 of ASTM standard F606-13,  $A_t$  is the stress area calculated from the minor thread diameter in the threaded length,  $d$  is the minor thread diameter,  $l_s$  is the length of the shank of the bolt and  $l_t$  is the thread length. This provides the slope of the line for the bolt side of the joint diagram.

The values for the lengths and areas for the two bolts are very similar. The length of the shank,  $l_s$ , is 1.5 inches for A286 and 1.28 for the titanium 6-4. The length of the threaded region,  $l_t$ , is 0.544 inches for A286 and 0.725 for the titanium 6-4. The minor diameter for 1/4"-28 UNJF thread is 0.2062 inches. The area of the shank will be calculated following equation 1 of ASTM STD F606-13 [32] for stress area which is as follows:

$$A_s = 0.7854[D - 0.9743/n]^2 \quad (3)$$

where, D is nominal diameter of the bolt and  $n$  is the number of threads per inch. This calculation produces an area of  $0.0364 \text{ in}^2$ . The area of the thread will just use the area of a circle equation with the minor thread diameter. This produces a value for thread area,  $A_t$ , of  $0.0334 \text{ in}^2$ . From the data collected the elastic modulus, E, of A286 is 16,990 ksi and 12,932 ksi for titanium 6-4.

One sample calculation is carried out below for A286:

$$\frac{1}{K_B} = \frac{1}{16,990,000} \left( \frac{0.4(0.2062)}{0.0364} + \frac{1.5}{0.0364} + \frac{0.045}{0.0334} + \frac{0.4(0.2062)}{0.0334} \right) \quad (4)$$

$$\frac{1}{K_B} = \frac{1}{16,990,000} (2.266 + 41.21 + 1.347 + 2.469)$$

$$\frac{1}{K_B} = \frac{47.292}{16,990,000}$$

Be sure to account for the assembled joint dimensions for the length of the threaded portion taking into account the nut and washer dimensions along with length for full thread engagement.

Once calculations for the spring constant are carried out they yield values of around  $363,000 \text{ lb/in.}$  for the A286 bolt and  $280,000 \text{ lb/in.}$  for the titanium 6-4 fastener rounded to three significant figures for calculations and graphing purposes.

## D.2 Joint Spring Constant

As stated previously determining the joint spring constant is more complex due to uncertainties in finding the true location of the loading planes. The same basic equation for spring constant is used from the modified Hooke's Law equation but a substitute area is applied based on the diameter of the joint compared to the area of the bolt head being used with the fastener. Three different area examples are shown and the one chosen is what is thought to be the



most applicable with the joint being equal to or greater than three times the diameter of the bolt head. This area formula is below:

$$A_s = \frac{\pi}{4} [(D_H + 0.1l_j)^2 - D_h^2] \quad (5)$$

where,  $D_H$  is Diameter of the bolt head,  $l_j$  is the length of the joint, and  $D_h$  is the diameter of the hole. The bolt heads of the two fasteners are almost identical and the A286 was taken for use in the calculation of 0.51 inches diameter. The A286 bolt was also taken to find a reasonable length of the joint. The total length is 2.03 inches from the base of the head to the end of the bolt. Based on NASA 5020 the full thread engagement is two times the pitch of the bolt so for these fasteners it came out to be 0.0714 inches and was rounded up to 0.08. Next a sample 12-point head nut was looked up which had a thickness of 0.375 inches and finally a washer was looked up and a thickness of 0.06 inches was found. After subtracting these thicknesses off the length of the bolt, along with another washer under the head, a joint thickness of 1.425 inches was arrived at for the examples. A hole size of 0.253 inches was decided on as an acceptable tolerance for a 0.25 inch bolt to fit in. Calculating the area with these variable results in an area of  $0.284 \text{ in}^2$ .

The joint spring equation is as follows and is from the Meyer's paper. The same basic equation is how Equation 1 was derived for the bolt's spring constant.

$$K_j = \frac{EA_s}{l_j} \quad (6)$$

The final variable that needed to be found was a joint materials elastic modulus. Following the example in NASA STD-5020 again an aluminum alloy (Al-6061) is used as a sample joint material. Calculating the spring constant for this sample joint comes out too  $1,991,584 \text{ lbf/in.}$ . This value will also be rounded to three significant figures of 1,990,000.

## APPENDIX E: JOINT DIAGRAM CALCULATIONS

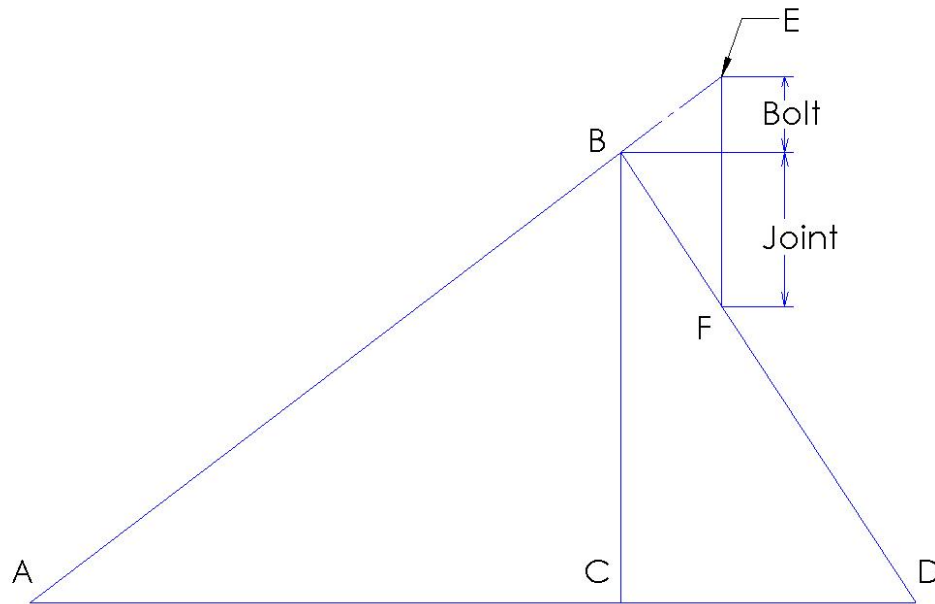


Figure AA: Joint Diagram Naming Convention

First, the equations of the lines for the diagram with full loading planes under the head and nut are calculated. These calculations are mostly just spring constants which are listed in Table 5 and whose calculations are in Appendix A.1. Since the line for the bolt goes through the origin the equation is even more simplified since the line crosses the y-axis at zero. Plug in the preload for the loading scenario and find the x-coordinate. These (x,y) coordinates will be point B in the diagram and point C is directly below.

Next, plug the point B values into the equation for the joint line to find the location which that line will cross the y-axis. Once the y-intercept is calculated the equation for the line of the joint is complete. Point D can now be found by setting this line equation equal to zero and finding the x-coordinate. These coordinates however are for the loading plane below the head and nut of the bolt.

To change these to half loading planes as in the majority of the examples subtract the x-coordinate from Point C from the x-coordinate from Point D and divide them by two. Add this number to the x-coordinate of point B and C and now the new coordinates for half loading planes are complete. This new x-coordinate will be where the preload line lies on. Point D stays in the same location and preload does not change. The length of the joint is simply rearranged so that the part taken up from the joint is cut in half.

Now that the slopes of the lines have changed the new line equations must be calculated. The slope for the bolt will be done first. Since the preload did not change that is the y-coordinate and the new location of the preload line is taken as the x-coordinate. Since the bolt line goes through the origin there is no y-intercept term. Calculating the slope from these two points gives you the new line equation for the bolt. Next, the slope of the joint equation needs to be found. The two sets of points to use are where the line crosses the x-axis and where it touches the top of the preload line. Dividing the difference in the y-coordinates over the x-coordinates will provide you with the slope. Using this slope and either one of the previous points will give the new y-intercept for this line. The new line equation for the joint is now complete.

External loading is the final step to complete the joint diagram. The length of this line is known because as stated previously it is set to be half of the preload. Setting the equations for the line of the bolt and joint equal to this external load and solving for x is how to find the location

where the external load will be located. This ensures that the top of the external load line lies on the extension of the bolt line and the bottom of this line lies on the joint line. Now that the x-coordinate where the external load will be applied is known the y-coordinates need to be found. Simply plug in that x-coordinate to the line equation for the bolt and joint and you have the (x,y) coordinates for Point E and F.

## APPENDIX F: OTHER JOINT DIAGRAM EXAMPLES

The figures in this appendix were not as notable as those presented in Chapter 5. They are joint diagram examples in which there is safety margin after the joint has separated. From any of the following 40% preload examples it can be seen that the external load does not have to grow by much to get to the point of joint separation. The first four are lower bound (40% preload) cases for the 65% preload examples. Since the half and full loading plane joint diagram examples show that at 65% the fasteners will perform safely the 40% cases will as well. The information still wanted to be presented for completeness however so they appear in this appendix.

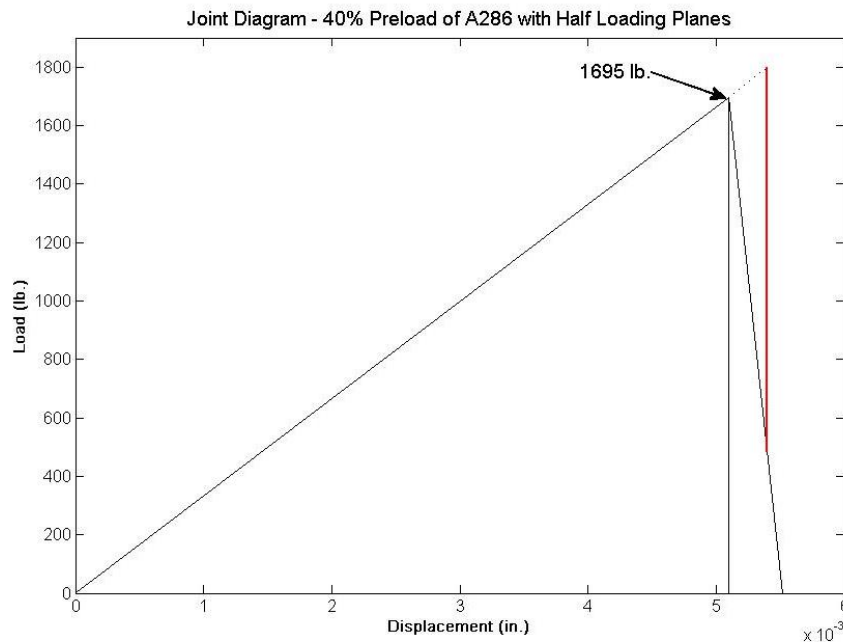


Figure BB: 40% Preload of A286 Joint Diagram

Figure BB is the joint diagram example for the lower uncertainty case of 65% preload. This means 40% (65%-25% uncertainty) preload is applied which is 1695 lb. as can be seen in the figure. The max load seen by the bolt with the external load of 1377 lb. applied is 1800 lb. When the joint separated the load seen by the fastener will be 2,004 lb. With a safety factor of 1.4 the safe load then is 2,805 lb. which is well below the minimum tensile strength seen by the A286 fasteners of 5,906 lb. The 40% preload case will perform safely after joint separation.

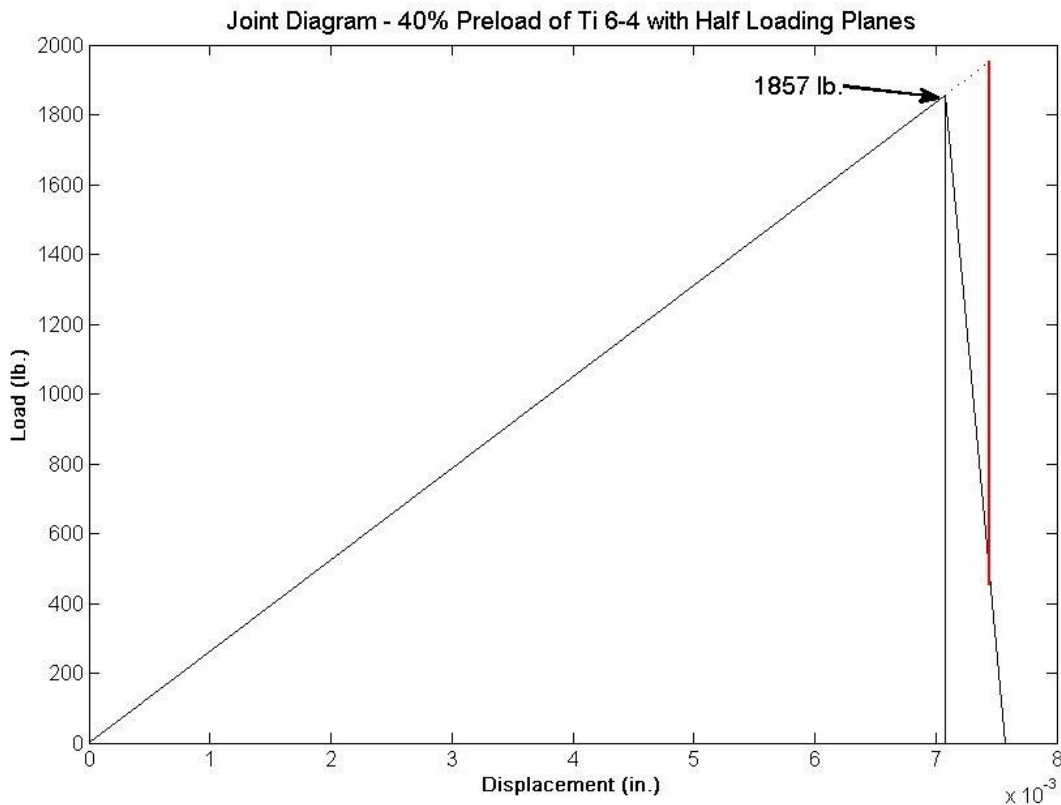


Figure CC: 40% Preload of Titanium 6-4 Joint Diagram

Figure CC shows the joint diagram example for titanium 6-4 with the lower limit of uncertainty of 65% preload. This 40% preload is 1,857 lb. as can be seen in the graph. The highest load seen by the fastener in use with the external load of 1,509 lb. will be 1,955 lb. The

joint will separate before rupture in this example and at separation the bolt will see 2,120 lb. With a 40% safety factor the value is brought to 2,967 lb. which is below the 6,035 lb. minimum tensile load carried by the bolts in testing. This means that titanium 6-4 will perform safely even after joint separation occurs.

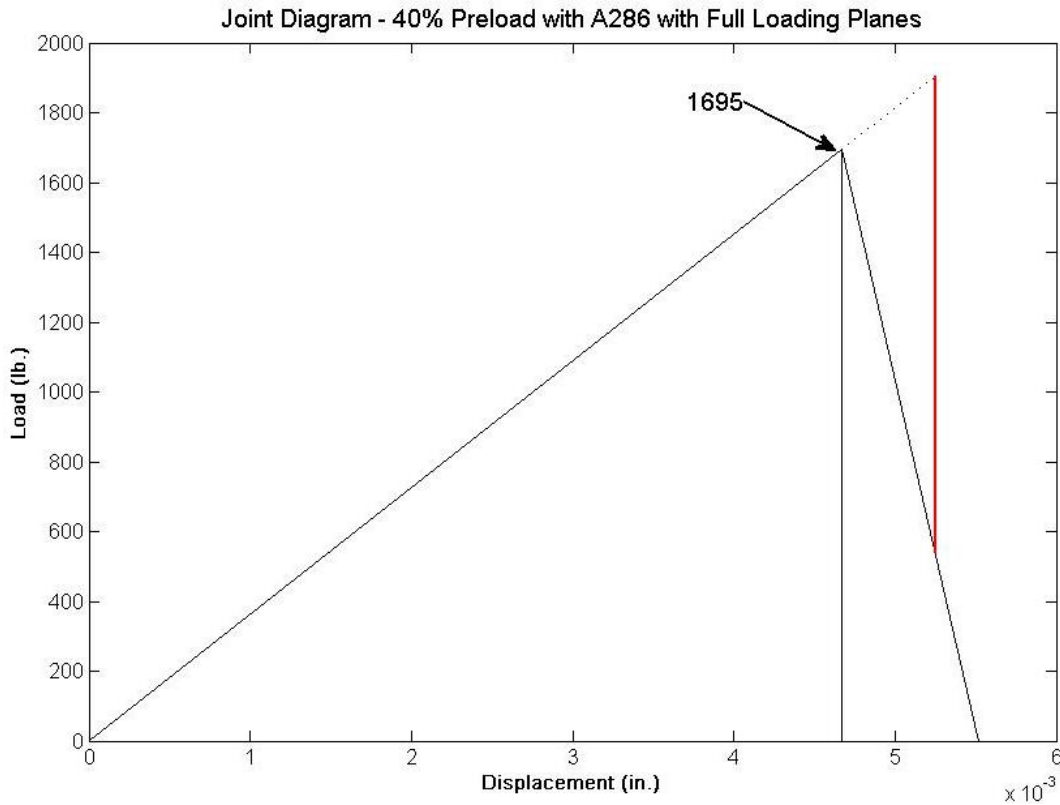


Figure DD: 40% Preload of A286 Joint Diagram - Full Loading Planes

As can be seen in Figure DD the preload for the A286 40% joint diagram example is 1,695lb. The maximum load seen by the bolt in use in this example will be 1906 lb. Upon joint separation the bolt will see a load of 2,004 lb. and with a safety factor of 40% the safe load will be 2,805 lb. This is below the minimum tensile strength seen by the A286 test specimens in this research of 5,906 lb. which means that this joint diagram example will safely perform with the conditions it is subjected to.

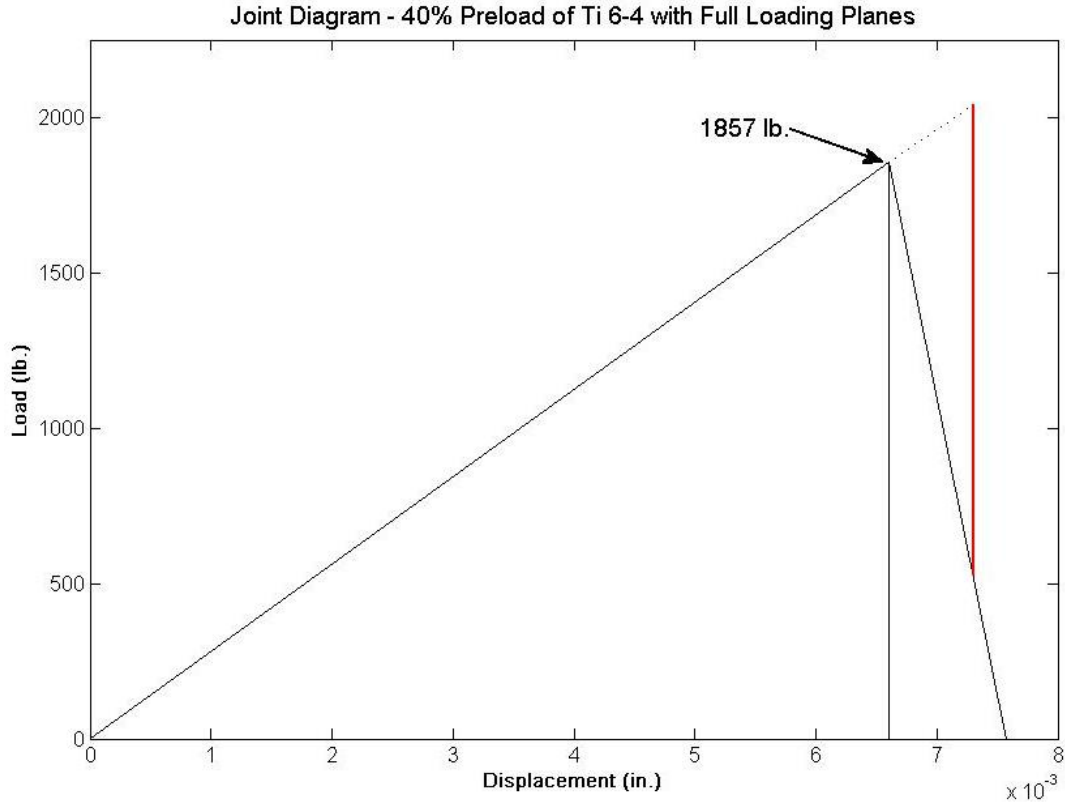


Figure EE: 40% Preload of Titanium 6-4 Joint Diagram - Full Loading Planes

Figure EE shows the 40% preload of titanium 6-4 which is the lower limit of uncertainty of the 65% preload with full loading planes. This produces a preload of 1,857 lb. as can be seen in the figure. The max load seen by the bolt in use is 2,043 lb. The load at separation then is 2,120 lb. and when a safety factor of 40% is applied the value is brought to 2,967 lb. which is below the minimum tensile strength of 6,035 lb. seen in testing for this research.



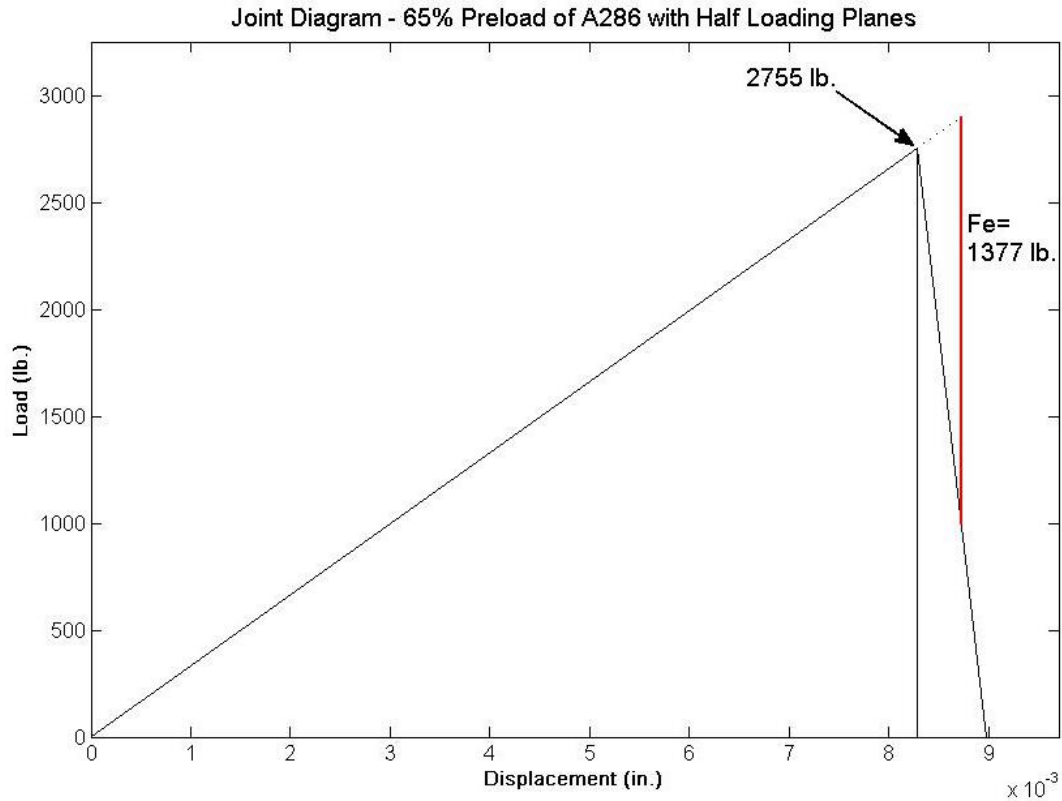


Figure FF: 65% Preload of A286 Joint Diagram

Figure FF is the lower bound (90%-25% uncertainty) of the 90% preload examples. The preload seen by the bolt is 65% of the minimum yield seen by the testing conducted for this thesis but the external load is based off of 90% preloading. This example will have joint separation before rupture and at when that occurs the bolt will see the full load of 3,256 lb. With a 40% safety margin this value is brought to 4,558 lb. which is below the minimum tensile strength seen in testing for A286 of 5,906lb. This joint diagram example would be deemed safe to use.

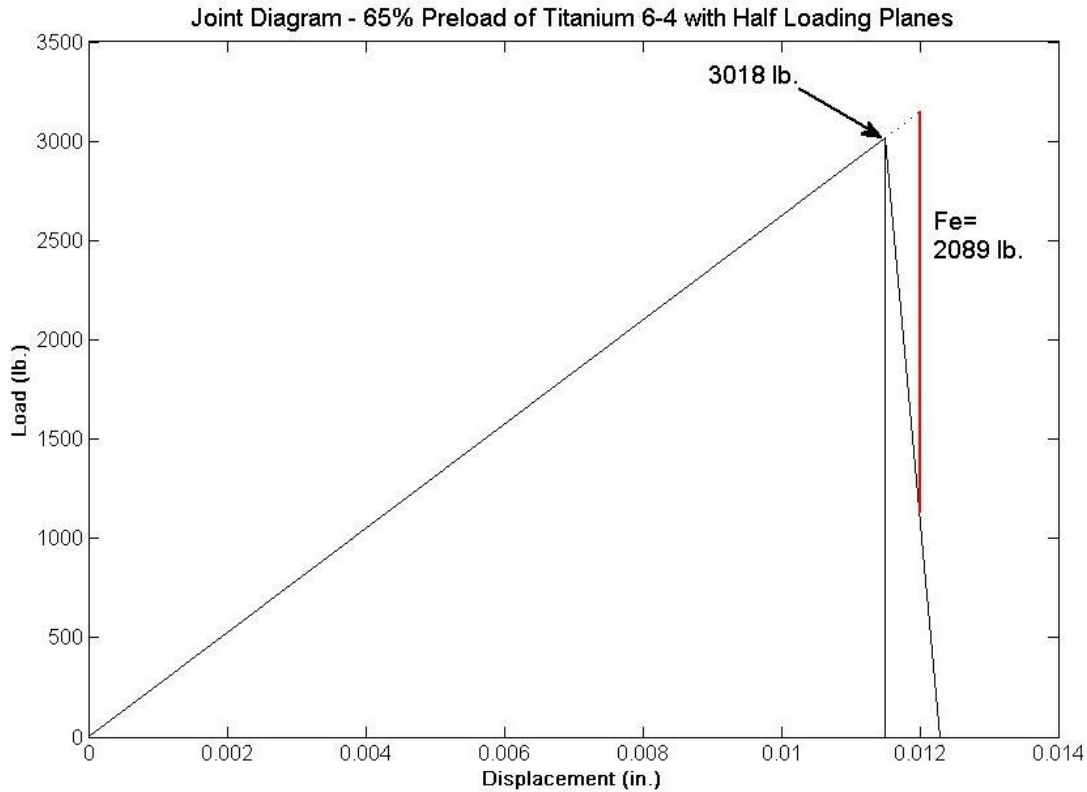


Figure GG: 65% Preload of Titanium 6-4 Joint Diagram

Figure GG shows the lower uncertainty bound for the 90% preload case which is 65% preload with the external load based off of 90% preload. This puts 3018 lb. preload on the bolt. This joint diagram example will separate before rupture and when separation occurs the load seen by the bolt will be 3,444lb. With a safety factor of 1.4 this value becomes 4,821 lb. which is below the minimum tensile strength seen in testing for titanium 6-4 of 6,035 lb. so this example is safe to use.

The final two examples for this Appendix will be the case of 65% nominal preload with 25% Torque-preload uncertainty. This means the bolt will be subjected to 90% preload based on minimum yield strength of the material seen in testing and an external load which is half of the

65% yield value. These will be switching back to half loading planes like the 65% examples from Section 5.8.

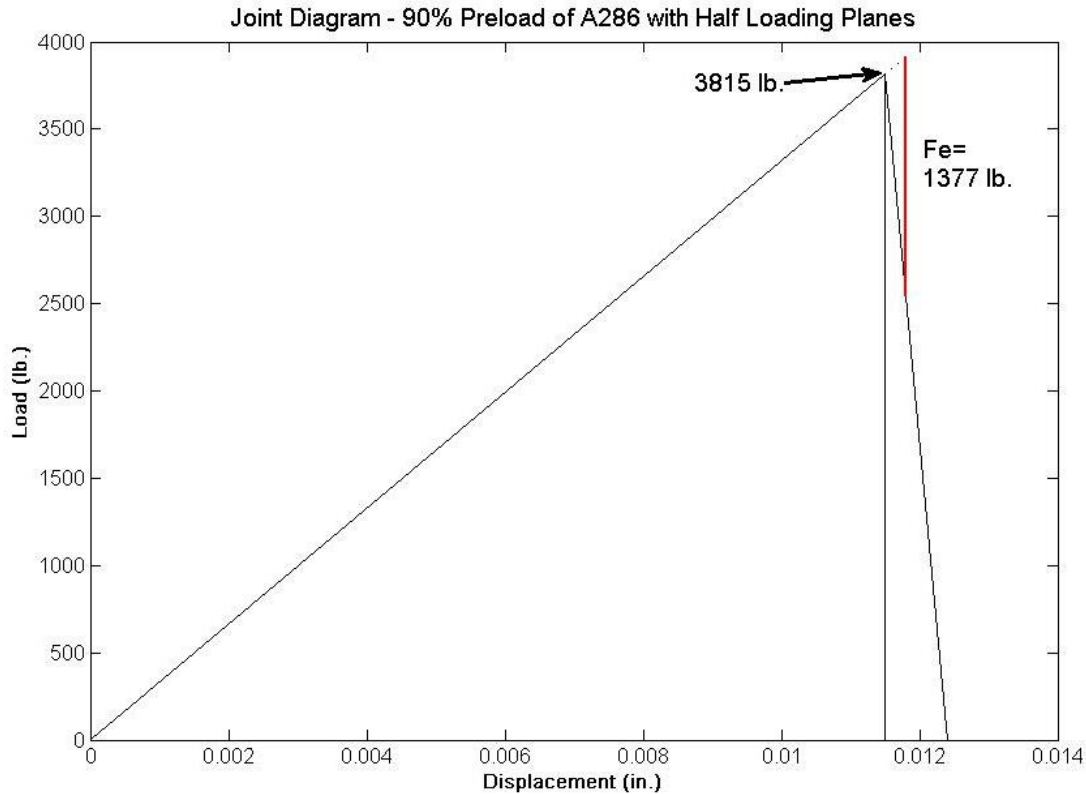


Figure HH: 90% Preload (65%+25% Uncertainty) of A286 Joint Diagram

As shown the external load for the joint diagram in Figure HH is the same as that in Section 5.8 because even though the preload is 90% this example is based off of 65% nominal preload. The max load the bolt will see in use is 3,915 lb. This example will separate before rupture and when separation occurs the bolt will see the full 4,501 lb. tensile load. If a 40% safety margin is applied the value is brought to 6,301 lb. which is above the 5,906 lb. minimum tensile load seen in the testing for this thesis. This mean that the bolt will not fail in use, however, the 40% safety margin is not met. If the margin is lowered to 20% however this bolt will be considered safe to use when the joint separates.

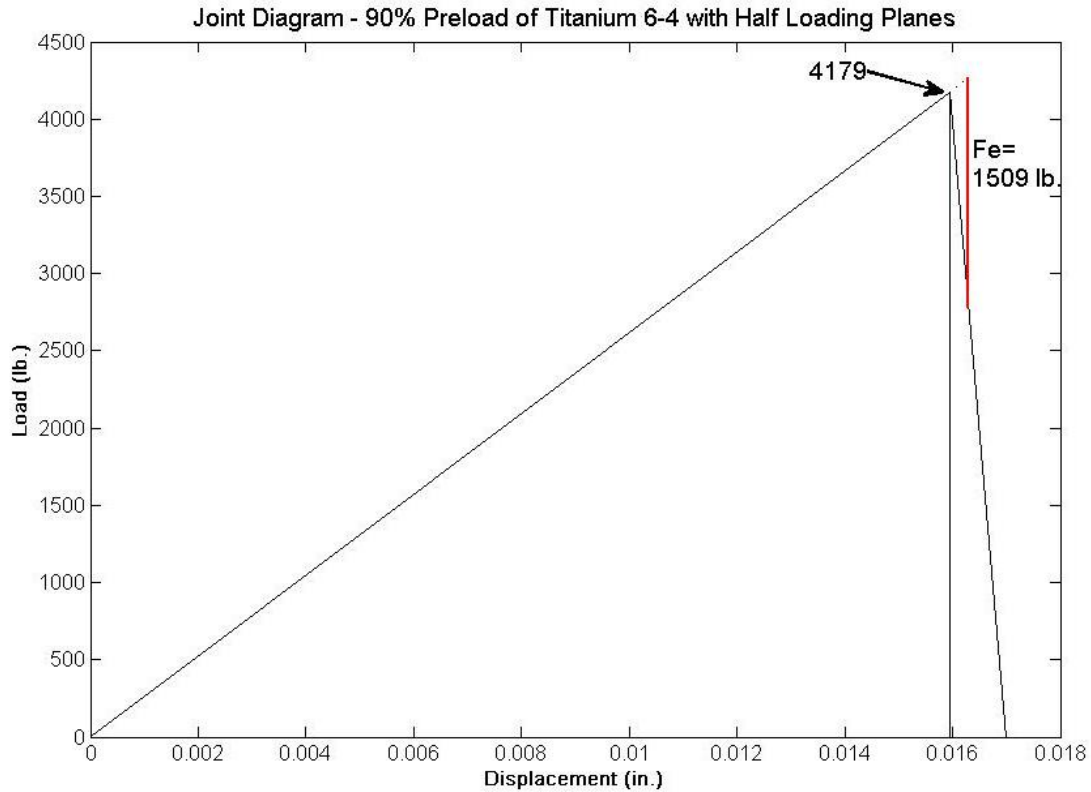


Figure II: 90% Preload (65%+25% Uncertainty) of Titanium 6-4 Joint Diagram

Like the joint diagram example before this in Figure II, Figure 65 represents 90% preload which is based off the upper end of uncertainty for the nominal 65% preload case. This means that the external load is based off of 65% preload. The maximum load the bolt sees in use will be 4,271 lb. This joint will separate before rupture and when separation occurs the bolt will see a tensile load of 4,760 lb. With a safety factor of 1.4 the safe load is then 6,664 lb. which is above the 6,035 lb. of minimum tensile strength of the bolts tested during research. If the safety margin is brought down to 20% however this bolt will be safe to use when joint separation occurs.

## APPENDIX G: COPYRIGHT PERMISSION

Below is permission to use Figure A

### SPRINGER LICENSE TERMS AND CONDITIONS

Jul 08, 2015

---

This is a License Agreement between Jarrod T Whittaker ("You") and Springer ("Springer") provided by Copyright Clearance Center ("CCC"). The license consists of your order details, the terms and conditions provided by Springer, and the payment terms and conditions.

**All payments must be made in full to CCC. For payment instructions, please see information listed at the bottom of this form.**

License Number	3660961110426
License date	Jul 02, 2015
Licensed content publisher	Springer
Licensed content publication	Springer eBook
Licensed content title	Metallurgy and Microstructure
Licensed content author	Russell Wanhill
Licensed content date	Jan 1, 2012
Type of Use	Thesis/Dissertation
Portion	Figures
Author of this Springer article	No
Order reference number	None
Original figure numbers	Figure 2.2
Title of your thesis / dissertation	Use and Use of Titanium Alloy and Stainless Steel Aerospace Fasteners
Expected completion date	Jul 2015
Estimated size(pages)	95
Total	0.00 USD

Terms and Conditions

#### Introduction

The publisher for this copyrighted material is Springer Science + Business Media. By clicking "accept" in connection with completing this licensing transaction, you agree that the following terms and conditions apply to this transaction (along with the Billing and Payment terms and conditions established by Copyright Clearance Center, Inc. ("CCC"), at the time that you opened your Rightslink account and that are available at any time at <http://myaccount.copyright.com>).